

Review

Overview and Status of the International Celestial Reference Frame as Realized by VLBI

Aletha de Witt ^{1,*}, Patrick Charlot ^{2,†}, David Gordon ^{3,†} and Christopher S. Jacobs ^{4,†}

- ¹ South African Radio Astronomy Observatory (SARAO), P.O. Box 443, Krugersdorp 1740, South Africa
² Laboratoire d'astrophysique de Bordeaux, Université de Bordeaux, CNRS, B18N, Allée Geoffroy Saint-Hilaire, 33615 Pessac, France; patrick.charlot@u-bordeaux.fr
³ U.S. Naval Observatory, 3450 Massachusetts Ave NW, Washington, DC 20392, USA; david.gordon126.civ@us.navy.mil
⁴ Jet Propulsion Laboratory, California Institute of Technology, 4800 Oak Grove Drive, Pasadena, CA 91109, USA; christopher.s.jacobs@jpl.nasa.gov
* Correspondence: alet@hartrao.ac.za
† These authors contributed equally to this work.

Abstract: Accurate measurement of angular positions on the sky requires a well-defined system of reference that is realized with accessible objects. The purpose of this study is to review the international standard realization of such a system, the International Celestial Reference Frame (ICRF). The ICRF uses the Very Long Baseline Interferometry (VLBI) technique as it has the highest resolution of any current astrometric technique for reference frames in order to observe Active Galactic Nuclei (AGN) which are at such great distances (typical redshift ~ 1) that there is currently no observed parallax or proper motion of these objects thus giving the frame excellent stability. We briefly review the history of the transition from the Fundamental Katalog 5 (FK5) optical frame to VLBI-based frames with attention to each of the three generations: ICRF-1, ICRF-2, and ICRF-3. We present some of the more prominent applications of the ICRF and outline the methods used to construct the ICRF. Next we discuss in more detail the current standard ICRF-3—which is the first frame to be realized at multiple wavelengths (S/X, K, X/Ka-bands)—including an estimate of its accuracy and limiting errors. We conclude with an overview of future plans for improving the ICRF.

Keywords: radio interferometry; astrometry; active galactic nuclei; ICRF



Citation: de Witt, A.; Charlot, P.; Gordon, D.; Jacobs, C.S. Overview and Status of the International Celestial Reference Frame as Realized by VLBI. *Universe* **2022**, *8*, 374. <https://doi.org/10.3390/universe8070374>

Academic Editor: Xue-Mei Deng

Received: 14 May 2022

Accepted: 28 June 2022

Published: 7 July 2022

Publisher's Note: MDPI stays neutral with regard to jurisdictional claims in published maps and institutional affiliations.



Copyright: © 2022 by the authors. Licensee MDPI, Basel, Switzerland. This article is an open access article distributed under the terms and conditions of the Creative Commons Attribution (CC BY) license (<https://creativecommons.org/licenses/by/4.0/>).

1. Introduction

The International Celestial Reference Frame (ICRF) is based on the currently accepted International Celestial Reference System (ICRS) [1] and forms the basis for all positional astronomy in the radio domain. The first three generations of this frame have been built from high precision Very Long Baseline Interferometry (VLBI) astrometric measurements of positions of extragalactic radio sources (quasars and other radio-loud Active Galactic Nuclei, AGN), with each successive realization of the ICRF becoming more precise [2–4]. VLBI angular position accuracy has now improved to near the 100 micro-arcsecond (μas) level. Catalogues of positions of extragalactic radio sources with the highest precision, such as the ICRF, are crucial to many applications, such as determining the Earth's orientation in space [5], providing calibrator sources for astronomy [6–8], studying the motion of tectonic plates [9], and in spacecraft navigation [10]. The ICRF also contributes towards the realization of a Global Geodetic Reference Frame (GGRF) [11] for sustainable development, a resolution adopted by the United Nations in 2015 [12].

Preparing a candidate celestial reference frame (CRF) for consideration for adoption as an official ICRF is a major undertaking which relies on international collaboration involving considerable effort and major investment in organizational, operational, analysis, and research and development activities (e.g., [13]). Global networks of radio telescopes

acquire weekly to monthly geodetic and astrometric VLBI data which are then transferred to the correlators for processing and then distributed to the analysis centers. To create a CRF, analysts use specialized software (e.g., [14]) to solve for source coordinates from the observed VLBI delays from all of the available data from geodetic and astrometric VLBI observing sessions, using the latest geophysical and astronomical models in compliance with the latest conventions [15] that define the standard reference systems. Another step in creating a CRF is to identify a subset of the ‘best’ sources, called defining sources, which are then used to define the axes of the new CRF.

Both the original ICRF [2] and its successor, the ICRF-2 [3], are based on dual-frequency 2.3 (S-band) and 8.4 GHz (X-band) VLBI observations that have been conducted since the end of the 1970s. A new realization, the ICRF-3 [4], was adopted by the International Astronomical Union (IAU) during its XXXth General Assembly in August 2018 [16] and has replaced the ICRF-2 as of 1 January 2019. The ICRF-3 is based on nearly 40 years of VLBI data at the standard S/X frequencies, along with observations at 24 GHz (K-band) and at 8.4 and 32 GHz (X/Ka-band), making it the first multi-wavelength frame ever realized. The S/X component of the ICRF-3 contains positions for 4536 sources—more than 1000 additional sources and more than a factor of three improvement in precision over the ICRF-2. In addition, a new set of 303 uniformly distributed defining sources, with very precise positions and fairly compact source structure, were selected to define the axes of the ICRF-3. Another new feature of the ICRF-3 is the incorporation of a Galacto-centric acceleration correction [17].

The accuracy of all three (wavelength) components of the ICRF-3 is limited by systematic errors such as stochastic fluctuations in tropospheric delay [18] and clocks as well as non-pointlike source structure [19]. The biggest challenge in improving precision is the need for more uniform global network geometry: North–South baselines in order to improve the declination precision in the approximate range $-45^\circ < \delta < +45^\circ$ and more South–South baselines to improve the deep South ($\delta < -45^\circ$). The IAU recommendations on the ICRF-3 [16] require that appropriate measures be taken to maintain and improve the ICRF-3, at multiple radio frequencies and with specific efforts on the Southern Hemisphere. Continued observations and dedicated efforts to improve the ICRF-3 have already shown a considerable increase in source density and precision over all three components of the ICRF-3 [20,21].

Looking to the future, the international community is developing road maps for continued improvement of the ICRF, e.g., [4] (Section 8), and [22–24], in particular dedicated strategies to improve the astrometric observing programs in the South, ongoing efforts to monitor source structure [8,25–28] and to mitigate its effect on the measured astrometric source positions [19,29,30], and plans for a fully integrated multi-wavelength realization of the ICRF, including also the optical *Gaia* reference frame [31,32].

This paper provides an overview of the evolution of the ICRF, since before its formal inception in 1997 up to its current status followed by plans for future realizations. The history and evolution of CRFs are given in Section 2, and the many applications of CRFs in Section 3. Details of how to construct a CRF are given in Section 4. A summary of the ICRF-3 is given in Section 5, and a discussion of the accuracy and limiting errors of the ICRF-3 is given in Section 6. Details on future plans to maintain and improve the ICRF are given in Section 7.

2. The History of Celestial Reference Frames Realized from VLBI

The construction of celestial frames goes back to ancient times such as Hipparchus, the Greek, in the 2nd century B.C. The advent of radio CRFs—the subject of this paper—had to wait until the discovery of astronomical radio emissions in the early 1930s by Jansky [33] and the invention of the VLBI technique in the 1960s [34–39].

Cohen et al.’s 1968 paper [40] as well as histories from Ken Kellerman [41,42] and Barry Clark [43] make it clear that even very early in the history of VLBI there were those who appreciated the potential of VLBI for milliarcsecond (mas) level astrometry. From 1972

to 1984, early astrometric results on compact extragalactic radio sources started to appear in the literature [44–49].

For many years the IAU's fundamental CRFs were based on optical observations of galactic stars. These frames were called 'Fundamental Catalogs' and they were labeled starting with FK1 and ending with the FK5 in 1988 [50] by which time it had become clear that the proper motions of stars in our galaxy were increasingly a limitation on the stability of the IAU's fundamental CRF.

During the second half of that same decade, VLBI had begun to produce high accuracy (mas) positions of extragalactic radio sources (e.g., [51–53]). These frames were typically oriented based on lunar occultations of 3C273B, which placed that quasar on the equator and equinox system of the Earth's orbit [54].

International coordination of VLBI CRFs began in the 1980s under the leadership first of the Bureau International de l'Heure (BIH) [55] and then the International Earth Rotation Service (IERS) [56–61]. In fact, the conventional orientation of the ICRF originates from the IERS frames; the small variations in orientation in the IERS frames until final convergence are summarized in [1].

In order to formalize the work started at the IERS, the IAU adopted a series of resolutions in the late 1980s and 1990s which laid the foundation for moving the IAU's official CRF from optical catalogs based on galactic stars to extragalactic objects [62]. These are as follows:

- (1) The 1988 resolution C1 [63] called for the IAU fundamental frame to move from galactic stars (e.g., as used in the FK5 frame [50]) to extragalactic objects.
- (2) The 1991 resolution A4 [64] recommended a general relativistic framework using a solar system barycentric frame (item 6).
- (3) The 1994 resolution B5 [65] documented the first list of so-called 'defining sources' to be used to define the rotational orientation of the frame. This was done three years before the adoption of the ICRF-1 in order to allow the ICRF-1 solution to be frozen in 1995 and in turn to give time for the Hipparcos optical catalog to be aligned with the ICRF-1 radio frame [66].
- (4) The year 1997 saw a series of resolutions [67]:

B2 adopting the first ICRF realized with VLBI observations in the radio and Hipparcos observations in the optical.

B3 on the relativistic framework.

B4 on Non-rigid earth theory for nutations.

B5 ICRS and Hipparcos.

B6 Relativity in celestial mechanics and astrometry.

The ICRF-1 with its 608 sources (Figure 1, left) and a noise floor of 250 μ s was adopted by the IAU in 1997 [2]. Soon after, the International VLBI Service for Geodesy and Astrometry (IVS) was organized to coordinate continued S/X observations, processing, and analysis amongst interested agencies around the world [13] in support of the celestial and terrestrial frames as well as the Earth Orientation Parameters (EOP). Official operations began in 1999.

By 2009, there was a significant enough increase in available data to warrant a second generation frame, the ICRF-2 [3], which had 3414 sources (Figure 1, right) and an estimated noise floor of 40 μ s. However, two-thirds of those sources were only sparsely observed in the first generation Very Long Baseline Array (VLBA) Calibrator Surveys (VCS) [6] with much larger position uncertainties than the other one-third of the sources. Consequentially, beginning in late 2009, the IVS Research and Development with the VLBA (RDV) sessions (VLBA plus 4–10 IVS stations) were used to re-observe some 12–15 VCS sources in each bi-monthly session, concentrating on the least observed sources. However the cadence and sensitivity of these had only a small impact on the overall precision of the VCS sources.

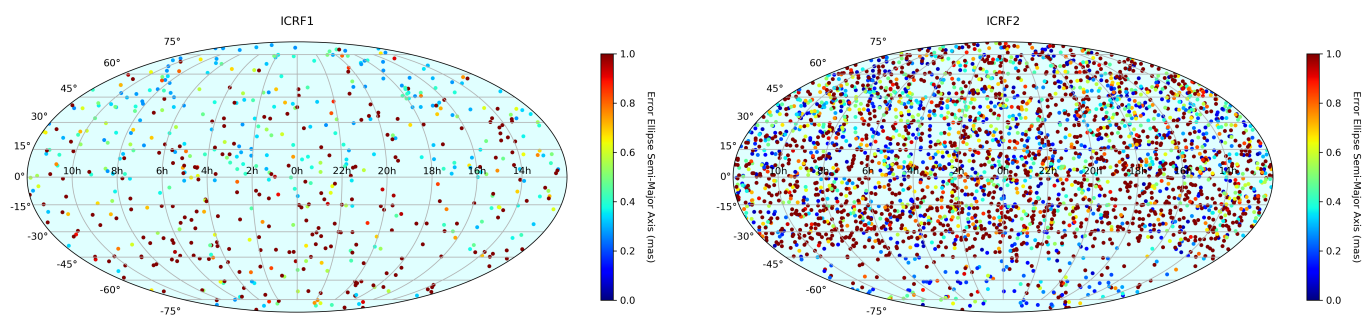


Figure 1. Sky distribution of the 608 sources in ICRF-1 (left panel) and 3414 sources in ICRF-2 (right panel). Each source is plotted as a dot color-coded according to its position uncertainty (defined as the semi-major axis of the error ellipse derived from the right ascension and declination uncertainties and correlation coefficients between the coordinates). The color scale ranges from 0 to 1 mas.

In 2012, work on the third generation ICRF began with the formation of an IAU working group. An emphasis was placed on increasing the observations of S/X survey sources starting with the VCS-II campaign in 2014–2016 [7], which improved survey source precision by about a factor of 5. From there the United States Naval Observatory (USNO) sponsored an ongoing series of survey observations contributing 25 additional VLBA S/X sessions by the March 2018 cutoff date of the ICRF-3. The ICRF-3 S/X cataloged 4536 sources with an estimated noise floor of 30 μ as. Table 1 summarizes the three generations of S/X-band ICRFs.

Table 1. Overview of the three generations of S/X-band ICRFs. The date gives the start of each frame as the IAU standard. N_{sources} gives the number of extragalactic radio sources in each S/X-band frame. The noise floor is the minimum realistic error based on internal repeatability studies. Note the trend of increasing number of sources and decreasing noise floor.

Frame	Date	N_{sources}	Noise Floor (μ as)
ICRF-1	1 January 1998	608	250
ICRF-2	1 January 2010	3414	40
ICRF-3	1 January 2019	4536	30

In addition to the S/X catalog, the ICRF-3 added two complementary catalogs at higher radio frequencies: K-band (24 GHz) and X/Ka-band (32 GHz). The motivation for augmenting S/X work with K-band and X/Ka-band was based on several factors. For one, S/X observations are becoming increasingly difficult due to increasing Radio Frequency Interference (RFI) at S-band. In fact, many of the next generation VLBI Global Observing System (VGOS) antennas may not support the S-band spectrum (≈ 2 – 3 GHz). There is also concern that source structure limits the accuracy and stability at S/X-band. On the positive side, source jets often have steep spectra causing the jet to fade with increasing frequency thus K- and X/Ka-band sources often have reduced source structure [28,68]. Ka-band has the added benefit of enabling spacecraft tracking at that frequency where telemetry bandwidth is higher than at X-band.

From 2002 to 2010, the initial work on higher frequencies began with VLBA sessions at K-band and Q-band (43 GHz) [69] motivated by a desire to explore higher frequencies while waiting for spacecraft tracking networks to install Ka-band. The early K-band results were very positive. However, sensitivity at Q-band was a serious limitation in those early experiments due to low data rates (128 Mbps) causing Q-band CRF work to be set aside until 2021 [28] when 4 Gbps was available.

In contrast, after only a few year hiatus, the K-band work was re-started in 2013 adding the baseline from Hartebeesthoek Radio Astronomy Observatory (HartRAO) 26 m antenna in South Africa, to the Hobart 26 m antenna in Tasmania, Australia. The addition of this all-southern baseline enabled full sky coverage at K-band for the first time [70]. Regular

VLBA observations resumed in 2015 including imaging of source structure [27]. We also note that K-band is the best of the three radio bands for observing near the Galactic plane due to its lower sensitivity to scattering from the Inter-Stellar Media (ISM). Thus K-band is important for studying objects in the plane of the Milky Way such as water masers [71] and the radio source at the Galactic center, SgrA* [72]. The ICRF-3 K-band catalog has 824 sources made from 56 sessions: 12 early VLBA (2002–2007) sessions, 28 more recent VLBA sessions plus 16 HartRAO–Hobart sessions.

In 2005, X/Ka-band work began driven by the need to track spacecraft at Ka-band starting with Mars Reconnaissance Orbiter (MRO) in that year [73]. In parallel, spacecraft networks soon began retiring S/X antennas: the National Aeronautics and Space Administration’s (NASA) Deep Space Station (DSS) 15 at Goldstone, CA, and DSS-45 at Tidbinbilla, Australia—with DSS-65 at Robledo, Spain, scheduled to be the next retirement. The Japan Aerospace Exploration Agency (JAXA) has replaced its 64 m S/X antenna at Usuda, Japan, with a 54 m X/Ka antenna 1.3 km away at Misasa. The European Space Agency (ESA) antenna at Malargüe, Argentina, never had S-band. Moreover, the number of S-band spacecraft missions has diminished significantly. We note that the move to Ka-band not only avoids S-band RFI, but it also greatly reduces plasma effects near the Sun where missions such as NASA’s Parker Solar Probe, ESA’s Bepi-Columbo, and JAXA’s Hayabusa-2 have traveled. For all these reasons, S/X work has been de-emphasized and X/Ka-band has become the focus for CRF work in the spacecraft tracking community. ESA joined the X/Ka-band effort in late 2012 with its 34 m antenna at Malargüe, Argentina, allowing full sky coverage at X/Ka for the first time [74]. JAXA joined in 2020 with its 54 m antenna at Misasa, Japan [75].

The ICRF-3 X/Ka-band catalog contains 678 sources observed on single baselines with the large NASA Deep Space Network (DSN) antennas and the ESA spacecraft tracking antenna at Malargüe, Argentina.

To summarize, the combined S/X, K, and X/Ka efforts were adopted as the ICRF-3 in 2018 [4,16] as the first multi-wavelength frame. That milestone paves the way for future integration of radio frames with the *Gaia* optical frame [31,76]—which, since 1 January 2022, is the official realization of the ICRS at optical wavelengths [32]. The story of the ICRF so far spans four decades from the first S/X observations in the late 1970s to the adoption of the ICRF-3 in 2018 with each successive ICRF realization taking about a decade. Having briefly reviewed the history of VLBI CRF work, we now turn to applications of those frames.

3. Applications of Celestial Reference Frames

A CRF provides fiducial points on the sky for measuring angles. The main advantage of VLBI versus artificial satellite techniques such as Global Navigation Satellite Systems (GNSS) and Doppler Orbitography by Radiopositioning Integrated by Satellite (DORIS) is that the ‘orbits’ of the VLBI sources are stable to better than a part per billion over time scales of decades using only two parameters to describe their position. This extreme stability of the CRF objects gives a corresponding stability to the many applications of VLBI.

What are these applications? For millennia travelers both on land and especially at sea used the stars to navigate by. We have now extended this idea to enable ‘sailing’ the solar system for exploring the planets. Related to that work, we use the radio sources as reference points against which the motion of the planets are tracked and thus improve our knowledge of the planetary ephemeris [77]. Even farther from home, the CRF enables differential astrometry of the position, parallax, and proper motions of objects in our galaxy such as water masers which trace out the spiral arms of our galaxy [71]. Calibrators from the CRF are also used to phase calibrate images of other extragalactic radio sources [78,79]. By observing changes in the apparent positions of extragalactic sources, we can also test the theories of special relativity (aberration) and general relativity via gravitational delay/‘bending’ [80]. Returning nearer to Earth, VLBI signals contribute to atmospheric studies by measuring the ionosphere and troposphere. Of course, the CRF is essential to geodesy which measures both motions of the stations (tidal motions, plate tectonics) [9]

as well as the orientation of the Earth in space [5]. VLBI is the premier technique for measuring UT1-UTC and nutation from which we get a deeper understanding of the interior of the Earth.

In deep space, there are no GNSS satellites with which to navigate. One has to rely on observations of naturally occurring objects such as quasars. Spacecraft angular positions are measured by doing a differential VLBI group delay measurement between an ICRF source and the spacecraft radio signal [10]. This data is combined with measurements of radial distance (range) and velocity (Doppler) to determine the complete position and velocity in three dimensions.

One of the key advantages that VLBI has over space-based missions, such as *Gaia* [81], is the capability to continue observations without any large temporal gaps (such as that occurring between space missions) for all VLBI products such as CRF, Terrestrial Reference Frame (TRF) [82,83], and EOP [5]. While our VLBI sources have no measurable parallax or proper motion, effects such as Galacto-centric acceleration [17] create effective proper motions that over the decades integrate up into significant position changes. The ICRF-3 is the first frame to model this Galacto-centric acceleration and refinements will surely be needed to maintain the long-term stability of the frame.

4. How to Construct a Celestial Reference Frame

A CRF is based on a celestial reference system (CRS), which gives the definitions and specifications of the system, such as its origin and axes, as well as what constants and models are to be used. The CRFs prior to 1991 were dynamical systems based on the Earth's motion in space, its mean equator and the dynamical equinox at some epoch. The FK5 catalog [50] was based on such a system. In 1988, the IAU decided to base its CRF on the precise coordinates of distant 'fixed' extragalactic objects [63]. The currently accepted ICRS is defined by the IERS in a kinematical sense with the origin at the solar system barycenter and with axes fixed with respect to distant objects in the Universe [1]. For continuity, the ICRS was initially aligned with the previous dynamical FK5 system by defining the principal plane to be close to the mean equator at J2000.0 and by defining the origin of right ascension by fixing the right ascension of the VLBI position of 3C273 to its FK5 value. The ICRS can be 'realized' by constructing a CRF of precise celestial coordinates of many 'fixed' sources in the sky. Distant quasars represent the ideal 'fixed' sources since they are so far away that they should not show any measurable proper motions and VLBI has been the only tool capable of very precise measurements until recently with *Gaia* [31,76]. The current ICRS was adopted by the IAU in 1997 and there have since been three ICRF radio realizations from VLBI measurements and two optical realizations: Hipparcos [67], and *Gaia*-CRF3 [31,32].

Creating a CRF with which to realize the ICRF is a major undertaking. ICRF-3 was created from a global least-squares solution of nearly 40 years of geodetic and astrometric VLBI observing sessions. Most of the ~6200 VLBI sessions used for ICRF-3 were approximately 24 hours in duration and involved from 2 to 32 VLBI stations. In a global solution, an analysis package, such as the CALC/SOLVE package, is used to make a least-squares solution between the observed baseline delays and modeled theoretical delays. The observed VLBI delays are the differences in arrival times of a wavefront at the two antennas of each baseline. Theoretical delays are computed using the latest geophysical and astronomical models in compliance with the latest IERS Conventions [15,84]. These models account for the effects of Earth rotation, precession/nutation, polar motion (wobble), solid Earth tides, ocean loading, Galacto-centric acceleration [17], the dry troposphere, and several other effects. Ionosphere corrections are computed from the delay differences between the two bands in dual band sessions, or by interpolating GNSS ionosphere maps in single frequency sessions. Global VLBI solutions normally solve for source coordinates as well as VLBI station positions and velocities, the five daily EOPs and residual atmosphere delays (mainly due to water vapor).

For ICRF-3, the resulting source catalog was kept in alignment with ICRF-2 by holding the 295 ICRF-2 defining sources to a no-net-rotation constraint [85] (Section 6, Appendix), in which any deviations of defining sources from their ICRF-2 positions would be averaged out over the other 294 defining sources. It has been found that the source position uncertainties from such solutions are underestimated because the software cannot take into account all the error sources and correlations between baselines. Therefore, the formal errors are first increased by 50% and then a noise floor value is added in an RSS sense. Noise floors can be estimated by doing solutions on subsets of the data and seeing how well the resulting source catalogs agree. For the ICRF-3 S/X catalog, noise floors of 30 μas in right ascension and declination were determined, down from the 40 μas of ICRF-2 and the 250 μas of ICRF-1 (Table 1).

Another step in the creation of a CRF is to select a set of ‘defining’ sources to define the axes of the new CRF. This set of sources is to be held to a no-net-rotation constraint in future solutions in order to prevent arbitrary rotations of the reference frame. Ideally, defining sources should be very stable in position, frequently observed and evenly distributed around the sky. The reality though is far from ideal. When choosing defining sources, source structure is an important criteria and only compact sources are chosen whenever possible.

Many of the ICRF sources exhibit spatially extended intrinsic structure that can introduce significant errors in the VLBI delay measurements [86] and instabilities in the individual source positions [87]. Ideally, the effects of source structure should be accounted for in the VLBI global solutions [19]. However, such modeling is facing many issues in practice, from temporal variability to frequency dependence, which makes the identification of an appropriate structure feature that is stable over time and frequency for every source not so easy [88]. Achieving this goal would require a more or less quasi-permanent ongoing imaging effort for all CRF sources.

Finally, for a new CRF to become the ‘International’ CRF, it must be adopted by the IAU [16,67,89]. This requires the writing and acceptance of formal IAU resolutions six months in advance. Lastly, the prospective ICRF needs to be made publicly available to the IAU community and then needs to be voted on and accepted by the IAU members at an IAU General Assembly business meeting.

5. Overview of the ICRF-3

The ICRF-3 [4] is based on nearly 40 years of VLBI data (1979–2018) at the standard S/X frequencies, along with observations at K-band and X/Ka-band that were initiated in the early/mid 2000s [69,90], making it the first multi-frequency frame ever realized. The data come from a total of 167 radio telescopes organized under the umbrella of the IVS, VLBA, and DSN, or through ad hoc VLBI networks in the early years. The geographical distribution of these telescopes is pictured in Figure 1 of the ICRF-3 publication [4]. The ICRF-3 contains positions for a total of 4536 sources at S/X-band (see the sky distribution in Figure 2), which is 1122 (about one-third) more sources than in the ICRF-2. The S/X-band positions are supplemented with independently estimated positions for 824 sources at K-band and 678 at X/Ka-band. In all, the frame comprises 4588 sources, 600 of which have positions available at the three frequency bands. Another new feature of the ICRF-3 is the incorporation of a Galacto-centric acceleration correction of 5.8 $\mu\text{as}/\text{year}$, estimated directly from the S/X-band data. This correction was mandatory due to the data span involved, as otherwise the effect induced would have caused deformations of the frame.

The noise floor in the individual ICRF-3 source coordinates is at a level of 30 μas , with a median position error at S/X-band of about 0.1 mas in right ascension and 0.2 mas in declination (Figure 2)—a factor of more than three improvement over the ICRF-2. This improvement results from the re-observation of all of the ICRF-2’s lower-accuracy VCS-type sources, as explained above. While the large number of survey sources dominates the error statistics, it must be emphasized that the S/X band catalog also includes a subset of roughly 500 sources, observed as part of the IVS programs, which have highly precise positions (uncertainties in the range of 30–60 μas). This subset manifests itself through a secondary

peak, next to the noise floor, in the histogram of position uncertainties plotted in Figure 2. The median positional precision at K band and X/Ka band approaches that at S/X band but remains a factor of 1.5–2 lower when comparing the $\alpha \cos \delta$ and δ uncertainties for the sources common to all three bands.

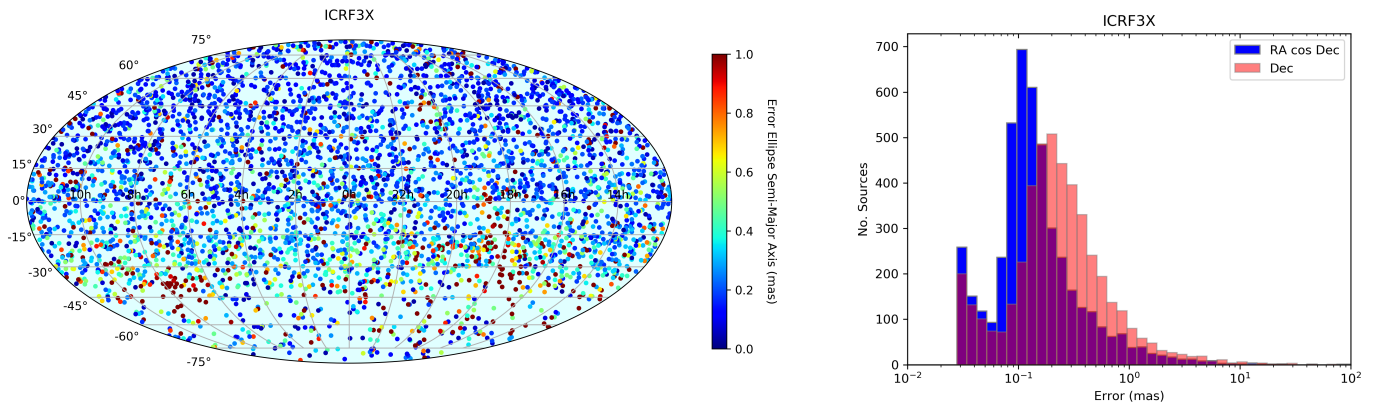


Figure 2. **Left:** Sky distribution of the 4536 sources in the ICRF-3 S/X frame. Each source is plotted as a dot color-coded according to its position uncertainty (defined as the semi-major axis of the error ellipse derived from the right ascension and declination uncertainties and correlation coefficients between the coordinates). The color scale ranges from 0 to 1 mas. **Right:** Distribution of coordinate uncertainties for the same 4536 sources. Right ascension is shown in blue, declination in salmon, and the superimposed portion in purple. Reproduced from [4].

A subset of 303 sources among the most observed ones at S/X-band have been picked out as defining sources and as such serve to define the axes of the ICRF-3. The selection of these sources was achieved by splitting the celestial sphere into equivalent sectors and identifying the most compact and stable source in each sector based on the available S/X-band data (leaving out the few sectors where no such sources were available). As a result of this selection process, the sky distribution of the ICRF-3 defining sources is fairly uniform (Figure 3, left panel). Furthermore, these sources, in their vast majority, have also very precise positions. Median uncertainties are 36 μ as for right ascension and 41 μ as for declination, which is very close to the noise floor (see the error distribution in Figure 3, right panel). They are also in general fairly compact, as illustrated by the sample of X-band images shown in Figure 4 for three such ICRF-3 defining sources.

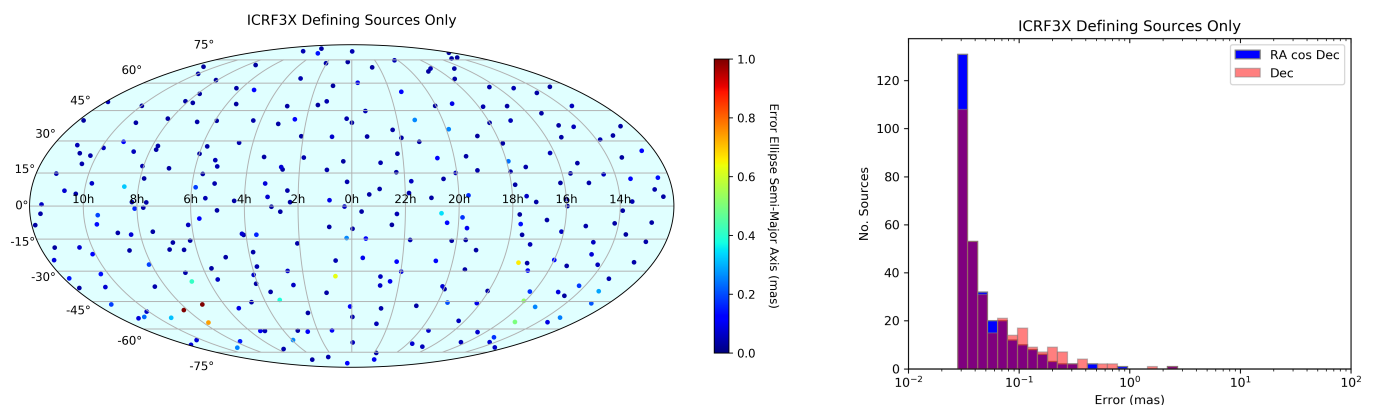


Figure 3. **Left:** Sky distribution of the 303 ICRF-3 defining sources. Each source is plotted as a dot color-coded according to its position uncertainty (defined as the semi-major axis of the error ellipse derived from the right ascension and declination uncertainties and correlation coefficients between the coordinates). The color scale ranges from 0 to 1 mas. **Right:** Distribution of coordinate uncertainties for these sources at S/X-band. Right ascension is shown in blue, declination in salmon, and the superimposed portion in purple. Reproduced from [4].

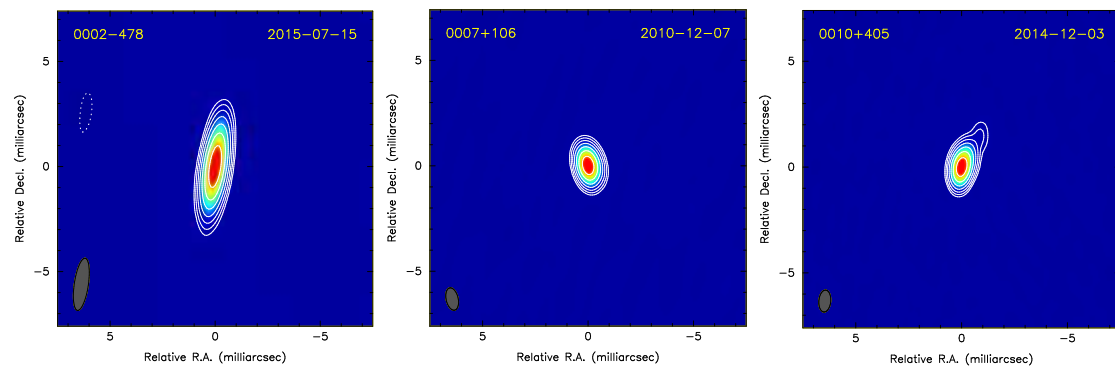


Figure 4. Very Long Baseline Interferometry (VLBI) maps at X-band for three ICRF-3 defining sources (0002-478, 0007+106, and 0010+405). Contour levels are drawn at $\pm 1, 2, 4, 8, 16, 32,$ and 64% of the peak brightness. These maps are from the Bordeaux VLBI Image Database, BVID [25]. See <https://bvid.astrophy.u-bordeaux.fr/> (accessed on 13 May 2022) for full details on the map parameters.

In general, the sources forming ICRF-3, however, are not as compact as those shown in Figure 4. They exhibit spatially extended brightness distributions that vary in both time and frequency. On VLBI scales, their morphology is usually characterized by single-sided jets that can extend over several mas, as illustrated by the sample of images at X and S bands shown in Figure 5. Due to the non-point-like nature of the sources, regular VLBI imaging sessions were initiated in the late 1990s [91] and indicators such as the structure index have been developed to assess the astrometric source suitability [92,93]. The monitoring of the sources through these sessions allows for tracking source structure variations and helps to further qualify the astrometric source suitability [94]. Altogether, these elements were essential in the selection process of the ICRF-3 defining sources.

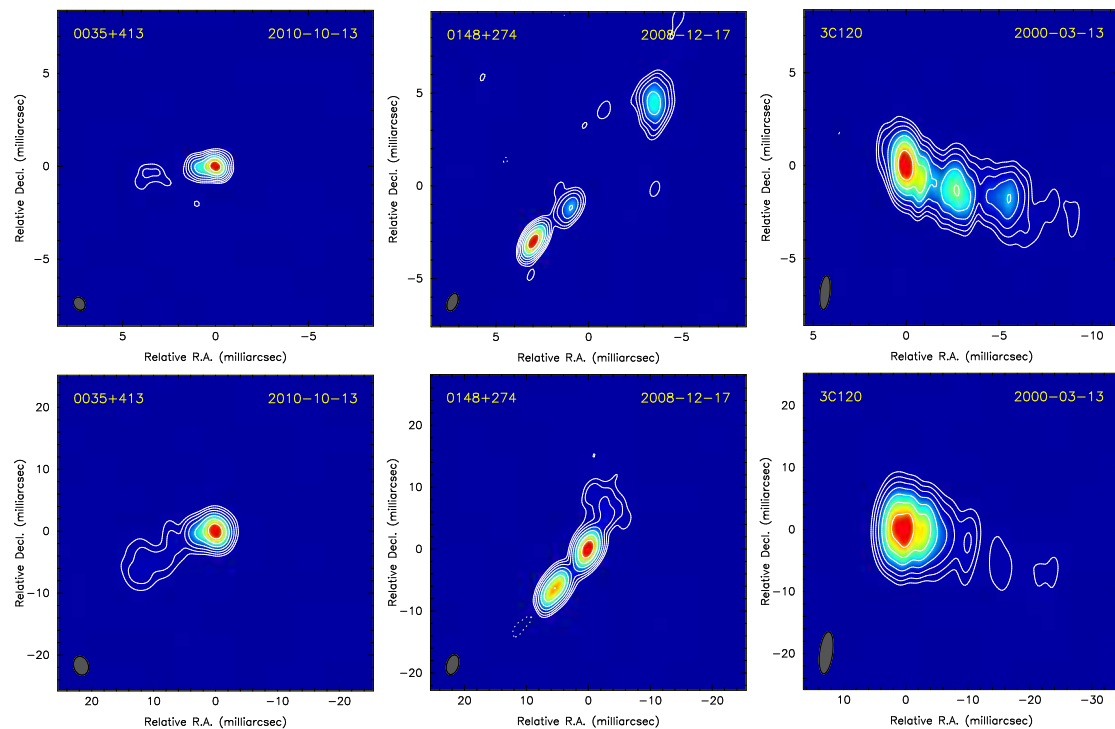


Figure 5. VLBI maps at X-band (upper sub-panels) and S-band (lower sub-panels) for three ICRF-3 non-defining sources showing single-sided jets (0035+413, 0148+274 and 0430+052). Contour levels are drawn at $\pm 1, 2, 4, 8, 16, 32,$ and 64% of the peak brightness. Note that the map scale at X-band and S-band is different. These maps are from the BVID [25]. See <https://bvid.astrophy.u-bordeaux.fr/> (accessed on 13 May 2022) for full details on the map parameters.

Comparison between the ICRF-3 S/X frame and the recently released *Gaia* CRF shows no relative global deformations between the two frames at the level of the ICRF-3 noise floor. On the other hand, significant ($>3\sigma$) offsets between the optical and radio positions are detected for more than 20% of the sources in common. Of particular interest is that these offsets occur predominantly for sources with extended VLBI morphologies. Significant positional offsets are also found within the radio band when comparing the K or X/Ka positions against the S/X positions. Although a smaller portion of the sources (5%) is concerned, here again sources with extended structure predominate among those showing offsets. Further studies have confirmed that the optical-to-radio offsets correlate with source structure [95], with the offset vectors preferentially oriented along the VLBI jet directions [96–100]. In all, there is thus now increasing evidence that the observed position differences between the bands are the manifestation of extended source structure, thus motivating the approach to estimate source positions at each band separately so that real astrophysical offsets between the bands can be preserved.

6. Current Status of the Celestial Reference Frame: Accuracy and Limiting Errors

The formal precision in all three components of the ICRF-3 (S/X, K, X/Ka) is quite good for well-observed sources, generally below 100 μs . So, the accuracy is limited by systematic errors. We quantify the systematics by inter-comparing the three independent S/X, K, and X/Ka frames. We also compare against the *Gaia* optical frame [76], which is an independent technique (optical versus radio, space versus ground, and pixel centroiding versus interferometry).

While our VLBI sources have no measurable parallax or proper motion, effects such as Galacto-centric acceleration create effective proper motions that over the decades integrate up into significant position changes. The ICRF-3 is the first frame to model this Galacto-centric acceleration and refinements will surely be needed to maintain the long-term stability of the frame. There are also long-standing issues from stochastic variations in clocks and tropospheres which will be difficult to eliminate entirely. On the analysis side, there are issues with modeling source structure as well as accounting for the correlated nature of stochastic errors when weighting solutions.

In addition to maintaining temporal continuity, our ICRF work needs more observations on North–South baselines to improve declinations. All three radio frames suffer from a deficit of long North–South baselines which can lead to declination precision being a factor of two or more worse than right ascension precision, depending on the region of the sky being observed.

Catalogs of compact extragalactic radio sources are generally weaker in the South by factors of 2 or more, in both density and precision. This is mainly because of the much smaller number of network stations in the South, compared to the North. Historically, approximately 80% of all antennas used in VLBI have been in the Northern Hemisphere. Even though the ICRF-3 showed significant improvement over the ICRF-2, the current S/X frame still shows deficiencies by factors of 2–3 in the South. More observations on North–South baselines are needed to improve declinations, and more southern stations are needed to observe sources in the deep South.

Since the spring 2018 cutoff date for sessions to be included in the ICRF-3, observations and analysis have continued with very positive results at S/X and K-bands [20], and at X/Ka-band [21]. Imaging work, to assess and monitor the astrometric source suitability, has also continued, and images of ICRF sources from astrometric VLBI observations at S, X, and K-bands are continuously updated, e.g., as part of the Bordeaux VLBI Image Database (BVID) [25,101], the Radio Fundamental Catalog (RFC) [102] of the Astrogeo Center, the USNO Fundamental Reference Image Data Archive (FRIDA) [26,103], and as part of the K-band CRF collaboration [27]. The current status, including the accuracy and frequency specific limiting errors, for each of the S/X, K, and X/Ka frames, are detailed below.

6.1. The S/X-Band Frame

The S/X frame has the most sources, but the distribution of observations is very uneven. Some 80% of the sources have been observed in fewer than 10 observing sessions. In contrast, 99 sources have been observed in 1000 or more sessions, the most observed source being OJ287 in over 4800 sessions. The S/X frame also has the most source structure issues, since source structure tends to decrease with increasing frequency (e.g., as shown in Figure 5).

Dedicated S/X astrometry observations received a significant boost in 2017 when the USNO began funding 50% of the VLBA's budget in exchange for up to 50% of the observing time. Twice monthly VLBA S/X astrometry sessions were made until mid-2019, and then have continued at a monthly cadence into the present, in support of the USNO mission. The sessions through spring 2018 were used to add more sources while also significantly improving the precision of existing sources for ICRF-3. Since ICRF-3, the VLBA S/X sessions have concentrated on re-observing the lesser-observed sources and on adding new sources, particularly along the ecliptic band. At present, this work has yielded an S/X catalog of ~5460 sources. Approximately half of the additional sources added since ICRF-3 are located within 7° of the ecliptic, thus approximately doubling the number of ICRF sources available for navigation of interplanetary spacecraft. Precision of the 4536 original ICRF-3 S/X sources has been improved by ~25% to ~95 μ as in right ascension and ~160 μ as in declination. Imaging of the VLBA S/X sessions is also being made at the USNO and will serve to characterize the structure of ~4500 sources at S/X band (e.g., [26]).

However, the VLBA can only observe down to around -45° declination. In order to improve the S/X frame in the deep South, starting in 2018 the sensitivity of the Southern IVS CRF observations was increased from 256 Mbps to 1 Gbps and the pool of sources was increased by a factor of two [24]. This in turn has already improved the source density and spatial coverage in the South, as well as the position accuracy of Southern sources, in both coordinates. The scheduling of these sessions was also optimized, using the most recently developed geodetic scheduling software VIESCHED++ [104], to allow for simultaneous astrometric and imaging observations in order to map the structure and evolution of the CRF sources in the deep South (e.g., [105]).

6.2. The K-Band Frame

The K-band has also benefited from the USNO's VLBA timeshare allocation. Approximately monthly K-band VLBA sessions have been made since January 2017 for astrometry and imaging. Moreover, approximately two dozen single baseline HartRAO–Hobart26 sessions have been run since ICRF-3, improving the full sky coverage at K-band. In order to improve the K-band declinations, a North–South baseline (from Spain to South Africa) has been started. First fringes were obtained in 2021 and full 24-hour observations are scheduled for mid-2022. The K-band reference frame currently has ~1.8 million observations, a nearly four-fold increase over the ICRF-3, and has added 211 sources for a total of 1035, a 25% increase over ICRF-3. Source precision has also improved considerably at K-band to ~45 μ as in right ascension and ~80 μ as in declination, or ~40% better for the original 824 sources. Current K-band source precision is now nearly as precise as at S/X for 1014 sources in common to both catalogs. The biggest issue for the K-band frame is the limited number of sessions and observations from the Southern Hemisphere. In spite of this, the distribution of sources at K-band is fairly even between the North and South, even though less than 1% of the observations are made from the Southern Hemisphere. At K-band, ionosphere calibrations are less than perfect, being based on GNSS ionosphere data [106] due to the lack of dual-band observations, but do not appear to produce systematic errors above the current noise floor of ~30 μ as.

To date, a total of 5879 K-band images of 731 ICRF-3 sources, from 28 VLBA sessions spanning from 2015 to 2018, have been produced [27]. The vast majority of sources are imaged at multiple epochs. Quantitative estimates of source strength, size, compactness, and jet direction as well as the temporal stability of these quantities were derived to aid

in characterizing the suitability of each as a reference source. A sample of three K-band images is shown in Figure 6.

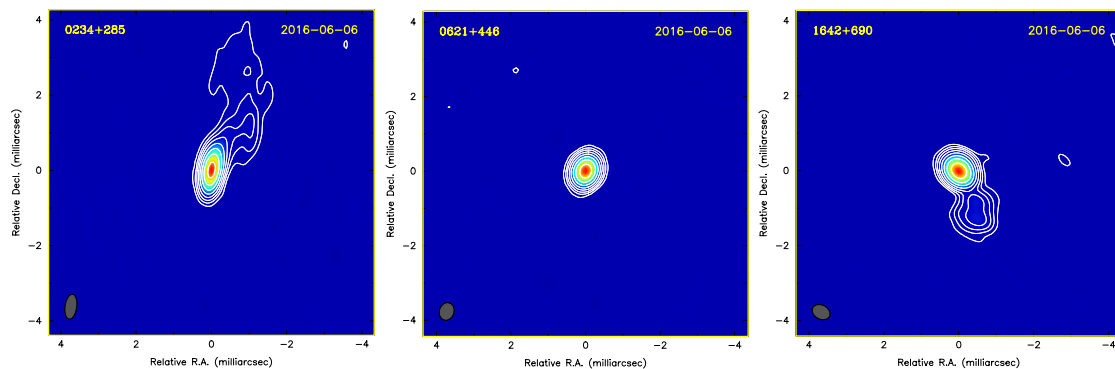


Figure 6. VLBA maps at K-band for three ICRF-3 sources (0234+285, 0621+446, and 1642+690) with compact structure or weak extended emission. The contour levels start at $3\times$ the background rms brightness level and increase by factors of 2 thereafter. The weak extended emission, visible only in the lower contour levels, has a small impact on the astrometry. See [27] (from which these maps are reproduced) for full details on the map parameters.

6.3. The X/Ka-Band Frame

The X/Ka frame has the largest zonal errors due to its reliance on just two baselines for $\sim 85\%$ of its data. As the X/Ka network geometry adds data from stations in Argentina and Japan, these errors are being reduced [21].

X/Ka (32 GHz) work with the combined NASA, ESA, and JAXA network has now produced 0.11 million observations. X/Ka-band sessions continue at an approximately three week cadence at 2 Gbps using a combined NASA, ESA, and JAXA network. As with the K-band program, the X/Ka program has added a long North–South baseline (Misasa, Japan, to Tidbinbilla, Australia) in order to improve declination accuracy [75]. Median source precision has improved considerably at X/Ka-band to 55, 75 μs in right ascension and declination, respectively. Accuracy is currently limited by a quadrupole 2.0 ‘magnetic’ distortion of $131 \pm 19 \mu\text{s}$. The large Z-dipole distortion seen in the ICRF-3 X/Ka [4] is now statistically insignificant as long as the full α - δ parameter covariances are accounted for [21].

7. Future Plans

It is essential that the CRF astrometric VLBI observing programs be continued and developed along the recommendations put forward in the IAU 2018 Resolution B2 on the ICRF-3 [16]. The IAU recommendations require that “appropriate measures be taken to continue to develop these programs, at multiple radio frequencies and with a specific effort on the Southern Hemisphere, to both maintain and improve the ICRF-3”. Many efforts are already underway to continue the maintenance of the ICRF, and the CRF community is developing a roadmap for the improvement of the ICRF. These efforts are closely aligned to the recommendations made by the ICRF-3 working group of the IAU on prospective astrometric VLBI observing programs and the future evolution of the ICRF [4] (Section 8). These recommendations are:

1. To devise a proper observing strategy to increase the source density and improve the source position accuracy of the S/X and K-band CRF’s in the far-south, and to reduce the systematics in the X/Ka-band frame.
2. To acquire more data and further increase the source position accuracy for ~ 3000 sources in the S/X-band frame that are observed in only a few sessions.
3. To include observations of optically bright ICRF-3 sources to strengthen the alignment between the radio VLBI and *Gaia* optical frames.

4. To closely monitor and image the defining sources in order to assess their astrometric stability and to track potential source structure changes.
5. To refine the underlying models, e.g., the determination of the solar system acceleration vector and the effects of source structure.
6. To explore alternate analysis configurations, e.g., multi-frequency analysis in which data sets at S/X, K, and X/Ka-band are processed together and to incorporate data from other space geodetic techniques, such as satellite and lunar laser ranging (SLR and LLR), GNSS, and DORIS systems, in the combination.

Monthly S/X astrometric observations on the VLBA, to add additional sources and improve the precision of existing ICRF-3 sources, will continue in support of the USNO mission. Imaging of VLBA sessions at S and X-band will also continue in order to characterize the source structure and its variation over time. Plans to increase the data rate of the S/X VLBA astrometric sessions from single-polarization 2 Gbps to dual-polarization 4 Gbps are being investigated. Efforts to improve the S/X frame in the deep South will also continue [24], e.g., adding more telescopes to existing Southern astrometric IVS sessions, and increasing the data rate of the deep South sessions from 1 Gbps to 2 Gbps. Running Southern observing programs at S/X-band that include some stations operating in single band (X) mode only, are also investigated: (1) to avoid severe S-band RFI issues at some stations and (2) to include large sensitive antennas that do not have dual-band capability, e.g., the 30 m Warkworth antenna in New Zealand. In addition, efforts to include more observations of defining sources in Southern sessions, as well as efforts to further optimize the networks and scheduling of the Southern sessions to allow for imaging, will continue.

Dedicated K-band astrometric observations will continue, with the goal of improving the quality of the observations. Imaging of VLBA sessions at K-band will continue and will be extended to include full Stokes polarization imaging. The fraction of polarized light may help to identify which component is the core and thus the point of reference for the source. Core components are often characterized by weak polarization that increases with larger distances from the jet base (e.g., [107,108]). The next challenge for K-band is to add North–South baselines longer than an Earth radius and, as noted earlier, full 24-hour sessions between the 40 m Yebes telescope in Spain and the 26 m HartRAO telescope in South Africa are scheduled to start in mid-2022. There are also plans to further increase the sensitivity of the K-band observations, e.g., to augment the VLBA with the 50-meter Large Millimeter Telescope (LMT) in Mexico [109]. The K-band frame remains weak in the South and options for adding more Southern stations to the existing K-band network are being investigated. Another challenge for K-band is the imperfect ionosphere calibrations based on GNSS data. Plans are underway to install geodetic GNSS stations at the five VLBA sites now lacking GNSS and thereby improve the ionosphere calibrations [106].

In the X/Ka program, work is underway to determine whether more sophisticated analysis using Kolmogorov spectrum correlated observation noise to account for tropospheric turbulence [18] will correct the quadrupole distortion. Furthermore, as noted earlier, the improved geometric diversity from the ESA and JAXA stations should help reduce distortions. In particular, since the dominant random and systematic errors are both a function of declination, the North–South baselines from Japan to Australia and from California to Argentina are expected to have the most impact.

Observations to explore the construction of CRFs at even higher radio frequencies, such as Q (43 GHz) and W (86 GHz) bands, are being investigated. At Q-band, a recent exploratory imaging-astrometry project to compare the structure of ICRF sources at S, X, K, and Q bands [28] showed promising results for the construction of a CRF at Q-band.

Efforts to observe ICRF-3 sources that are also seen in the optical band (i.e., detected by *Gaia*) will be pursued further, in particular by means of a dedicated and ongoing observing program conducted by the IVS at S/X band [110,111]. This program, which has run since 2013, should continue until the end of the *Gaia* mission (which is foreseen to be extended to 2025 at the end of the life time of the satellite). Plans to observe such sources in K-band sessions will also be implemented in the near future. Increasing the number of common

objects between radio and optical will depend largely on increasing the number of sources in the radio frame and therefore on having deeper VLBI observations. In this respect, the high sensitivity that the Square Kilometre Array (SKA) will have in its VLBI mode on long baselines (i.e., when observing jointly with VLBI arrays) at frequencies above 5 GHz will play an important role in detecting new, weaker radio sources and measuring their astrometric positions with sub-mas accuracy [112,113]. Ultimately, the SKA may be able to densify massively the radio frame, in particular by taking advantage of the possibilities of commensal observations, which would also multiply the number of radio counterparts to the sources that are comprised in the *Gaia* optical frame [114].

There are many ongoing efforts to image and monitor the ICRF sources on a regular basis and at multiple frequencies. Estimates of the source characteristics can be used to either filter out the sources with the least point-like structure or to apply structure corrections through modeling. There are also ongoing efforts, as mentioned previously, to study the frequency dependence of source positions and its correlation with source structure (e.g., [95,99,100]), which will be particularly useful in selecting defining sources for future multi-waveband realizations of the ICRF. In the four years since ICRF-3, a few defining sources have been found to be problematic, e.g., [27] (Section 7), and may need to be replaced when a new realization is made.

For now, the networks that will be targeted for CRF observations will be the legacy networks operating with legacy narrow-band systems. The level to which the broadband (2–14 GHz) VGOS [115] may contribute to the CRF is still to be evaluated—in particular, for how many sources may be observed, and for how to deal with source structure issues. Depending on the conclusions of this evaluation, VGOS observations may want to concentrate on a set of core sources, e.g., the ICRF-3 defining sources, ideally ultra-compact, and push their position accuracy to the limit, or cycle through a larger set of sources to start building a VGOS CRF. In any case, the VGOS CRF will not match any of the current S/X, K, or X/Ka band realizations because the source positions do not coincide at the different bands due to the changing source morphology as a function of frequency (e.g., [29]). However, for now, sessions observed in a mixed-mode configuration, including legacy systems and VGOS systems operating in the standard S/X-mode are being considered for IVS astrometric observations—in particular to densify the IVS network in the Southern Hemisphere. Initial tests to correlate and analyze mixed-mode sessions, using the Hobart, Katherine, and Yarragadee 12 m AuScope antennas in Australia were successful [116], and a more extensive test series, the Australian mixed-mode (AUM) sessions, was initiated in 2019 [117].

In the longer term, higher radio frequencies may benefit from a broad-band receiver being prototyped for the VLBA which would cover from 8 to 36 GHz [118]. This prototype is scheduled for testing at the Owens Valley VLBA site in mid-2022. If this system becomes operational, it has potential to enable simultaneous X/K (8/24) and X/Ka-band (8/32) observations. Each of the sub-bands (X, K, Ka) could be extended to as much as 4 GHz, thereby greatly improving sensitivity and group delay precision. Moreover, K-band would gain dual-band ionosphere calibrations for the first time thereby solving any ion calibration issues for VLBA observations.

Looking at the next stage, the future ICRF is likely to be multi-waveband, incorporating also the optical realization by *Gaia* into a fully unified multi-waveband frame integrating source positions in all available bands. To this end, a new IAU Working Group entitled ‘Multi-waveband ICRF’ has been created [119]. Areas of work (prior to producing such a frame) include agreeing on common values for the amplitude and direction of the Galactic acceleration vector, establishing common practices to align reference frames in different bands and to treat wavelength and time-dependent source positions, and defining a proper terminology for referring to individual (per wavelength) components of the reference frame. This future multi-waveband ICRF should be a valuable asset to further improve our understanding of the physics of the underlying objects.

8. Conclusions

The ICRF is the physical realization of the ICRS and comprises a catalog of precise positions of extragalactic radio sources observed by VLBI. The ICRF provides the basis for astrometry and deep space navigation and is essential for all space geodesy applications. Since the first realization of the ICRF by VLBI astrometry of extragalactic objects in 1997, the ICRF has evolved considerably. The most recent realization, the ICRF-3 was constructed using VLBI data acquired over nearly 40 years, and shows more than a factor of three improvement over the previous realization, the ICRF-2. The ICRF-3 is also the first multi-wavelength celestial reference frame ever generated and includes independent positions for sources at S/X-band, K-band, and X/Ka-band. The ICRF-3 was adopted by the IAU in August 2018 and is now the fundamental celestial reference frame to be used for all applications. Since 2018, considerable work has been done to maintain and further improve the ICRF-3, at all three frequency bands.

In the future, it will be necessary to continue to maintain and further increase the quality of the ICRF, which in turn will require a continued increase in the precision of the measurements and refinement of the methods and models used in the analysis. In order to achieve this, the current dedicated CRF observing programs must be assessed and one should determine whether it is possible to improve the observations with the available resources. Which sources, which network or network combinations, and which observing and scheduling strategy are the major points to be addressed in this respect. The second focus will be on alternate analysis techniques and the refinement of the modeling. Considering the effect of source structure in the modeling will become necessary. This will require imaging and monitoring of source structure, at all three frequency bands, which in itself is an enormous task.

Maintenance and continuous improvement of the ICRF requires a substantial investment from many individuals and institutions across the globe: the coordination centers and individuals responsible for planning and scheduling of the observations, each of the network stations and the operators that run the observations, the facilities that correlate the data, the analysis centers and many individuals that contribute to the models, the calibration and analysis of the data, and the evaluation of the results. No single person or entity can implement and monitor these programs on their own. Thus, we are thankful for the many scientists, engineers, and institutions that have contributed and continue to contribute to the great successes of the ICRF.

Author Contributions: Investigation, A.d.W., P.C., D.G. and C.S.J.; writing—original draft preparation, A.d.W., P.C., D.G. and C.S.J.; writing—review and editing, A.d.W., P.C., D.G. and C.S.J.; project administration, A.d.W. All authors have read and agreed to the published version of the manuscript.

Funding: AD was supported by the South African Radio Astronomy Observatory (SARAO), a facility of the National Research Foundation (NRF) of South Africa. PC's work was supported by the Observatoire Aquitain des Sciences de l'Univers (OASU) and the Programme National GRAM of CNRS/INSU with INP and IN2P3 co-funded by CNES. DG was supported by the U.S. Naval Observatory (USNO). CJ's work was supported by the Jet Propulsion Laboratory, California Institute of Technology, under a contract with the National Aeronautics and Space Administration (80NM0018D0004).

Institutional Review Board Statement: Not applicable.

Informed Consent Statement: Not applicable.

Data Availability Statement: The original ICRF-3 position data are publicly available at VizieR [120]. ICRF catalogs, updates, and ancillary data are also available at the ICRS Center at USNO <https://crf.usno.navy.mil/icrs> (accessed on 13 May 2022) and Paris Observatory <https://hpiers.obspm.fr/icrs-pc/newwww/index.php> (accessed on 13 May 2022).

Acknowledgments: The S/X results made extensive use of the International VLBI services (IVS) data set [115]. The S/X and K-band data sets also made extensive use of the VLBA [121] which is managed by the National Radio Astronomy Observatory (NRAO), funded by the National Science Foundation (NSF), and operated under cooperative agreement by Associated Universities. The authors gratefully

acknowledge use of the VLBA under the USNO's time allocation. This work supports USNO's ongoing research into the celestial reference frame and geodesy. The X/Ka data set made use of NASA's Deep Space Network [122], ESA's Deep Space Network [123], and JAXA's 54-meter Misasa station. This research has made use of material from the Bordeaux VLBI Image Database (BVID) [101]. We are grateful to Sébastien Lambert for providing ICRF-1 and ICRF-2 sky plots with a graphic display similar to the ICRF-3 ones.

Conflicts of Interest: The authors declare no conflict of interest. The funders had no role in the design of the study; in the collection, analyses, or interpretation of data; in the writing of the manuscript, or in the decision to publish the results.

Abbreviations

The following abbreviations are used in this manuscript:

AGN	Active Galactic Nuclei
AUM	Australian mixed-mode sessions
BIH	Bureau International de l'Heure
BVID	Bordeaux VLBI Image Database
CRF	Celestial Reference Frame
CRS	Celestial Reference System
DORIS	Doppler Orbitography by Radiopositioning Integrated by Satellite
DSN	Deep Space Network
DSS	Deep Space Station
EOP	Earth Orientation Parameters
ESA	European Space Agency
FK1	Fundamental Katalog 1
FK5	Fundamental Katalog 5
FRIDA	Fundamental Reference Image Data Archive
Gbps	Giga-bits per second
GGRF	Global Geodetic Reference Frame
GNSS	Global Navigation Satellite System
HartRAO	Hartebeesthoek Radio Astronomy Observatory
IAU	International Astronomical Union
ICRF	International Celestial Reference Frame
ICRS	International Celestial Reference System
IERS	International Earth Rotation Service
ISM	Inter-Stellar Media
IVS	International VLBI Service for Geodesy and Astrometry
JAXA	Japan Aerospace Exploration Agency
LLR	Lunar Laser Ranging
LMT	Large Millimeter Telescope
mas	milliarcsecond
Mbps	Mega-bits per second
MRO	Mars Reconnaissance Orbiter
μ as	micro-arcsecond
NASA	National Aeronautics and Space Administration
NRAO	National Radio Astronomy Observatory
NSF	National Science Foundation
RDV	Research and Development with the VLBA
RFC	Radio Fundamental Catalog
RFI	Radio Frequency Interference
SKA	Square Kilometre Array
SLR	Satellite Laser Ranging
TRF	Terrestrial Reference Frame
USNO	United States Naval Observatory
VCS	Very Long Baseline Array Calibrator Surveys
VLBA	Very Long Baseline Array
VGOS	VLBI Global Observing System
VLBI	Very Long Baseline Interferometry

References

1. Arias, E.F.; Charlot, P.; Feissel, M.; Lestrade, J.F. The extragalactic reference system of the International Earth Rotation Service, ICRS. *Astron. Astrophys.* **1995**, *303*, 604–608. Available online: <https://articles.adsabs.harvard.edu/pdf/1995A> (accessed on 13 May 2022).
2. Ma, C.; Arias, E.F.; Eubanks, T.M.; Fey, A.L.; Gontier, A.M.; Jacobs, C.S.; Sovers, O.J.; Archinal, B.A.; Charlot, P. The International Celestial Reference Frame by very long baseline interferometry. *Astron. J.* **1998**, *116*, 516. Available online: <https://iopscience.iop.org/article/10.1086/300408> (accessed on 13 May 2022). [[CrossRef](#)]
3. Fey, A.L.; Gordon, D.; Jacobs, C.S.; Ma, C.; Gaume, R.A.; Arias, E.F.; Bianco, G.; Boboltz, D.A.; Böckmann, S.; Bolotin, S.; et al. The Second Realization of the International Celestial Reference Frame by Very Long Baseline Interferometry. *Astron. J.* **2015**, *150*, 58. Available online: <https://iopscience.iop.org/article/10.1088/0004-6256/150/2/58/pdf> (accessed on 13 May 2022). [[CrossRef](#)]
4. Charlot, P.; Jacobs, C.S.; Gordon, D.; Lambert, S.; de Witt, A.; Böhm, J.; Fey, A.L.; Heinkelmann, R.; Skurikhina, E.; Titov, O.; et al. The third realization of the International Celestial Reference Frame by very long baseline interferometry. *Astron. Astrophys.* **2020**, *644*, A159. Available online: https://www.aanda.org/articles/aa/full_html/2020/12/aa38368-20/aa38368-20.html (accessed on 13 May 2022). [[CrossRef](#)]
5. Eubanks, T.M. Variations in the Orientation of the Earth. In *Contributions of Space Geodesy to Geodynamics: Earth Dynamics*; Smith, D.E., Turcotte, D.L., Eds.; Geodynamic Series; American Geophysical Union: Washington, DC, USA, 1993; Volume 24, p. 1. Available online: <https://agupubs.onlinelibrary.wiley.com/doi/pdf/10.1029/GD024> (accessed on 13 May 2022).
6. Beasley, A.J.; Gordon, D.; Peck, A.B.; Petrov, L.; MacMillan, D.S.; Fomalont, E.B.; Ma, C. The VLBA Calibrator Survey-VCS1. *Astrophys. J. Suppl. Ser.* **2002**, *141*, 13–21. Available online: <https://iopscience.iop.org/article/10.1086/339806> (accessed on 13 May 2022). [[CrossRef](#)]
7. Gordon, D.; Jacobs, C.; Beasley, A.; Peck, A.; Gaume, R.; Charlot, P.; Fey, A.; Ma, C.; Titov, O.; Boboltz, D. Second Epoch VLBA Calibrator Survey Observations: VCS-II. *Astron. J.* **2016**, *151*, 154. Available online: <https://iopscience.iop.org/article/10.3847/0004-6256/151/6/154/pdf> (accessed on 13 May 2022). [[CrossRef](#)]
8. Petrov, L.; de Witt, A.; Sadler, E.M.; Phillips, C.; Horiuchi, S. The Second LBA Calibrator Survey of southern compact extragalactic radio sources - LCS2. *Mon. Not. R. Astron. Soc.* **2019**, *485*, 88–101. Available online: <https://academic.oup.com/mnras/article/485/1/88/5301408> (accessed on 13 May 2022). [[CrossRef](#)]
9. Hellmers, H.; Bachmann, S.; Thaller, D.; Bloßfeld, M.; Seitz, M. Combined IVS contribution to the ITRF2020. In Proceedings of the EGU General Conference Abstracts, EGU21-10678, Virtual, 19–30 April 2021. Available online: <https://meetingorganizer.copernicus.org/EGU21/EGU21-10678.html> (accessed on 13 May 2022).
10. Thornton, C.L.; Border, J.S. Radiometric Tracking Techniques for Deep-Space Navigation. Deep-Space Communications and Navigation Series, Monograph 1, JPL Publication 00-11, Jet Propulsion Laboratory, California Institute of Technology. 2000. Available online: https://descanso.jpl.nasa.gov/monograph/series1/Descanso1_all.pdf (accessed on 13 May 2022).
11. Sub-Committee on Geodesy, Position Paper on Sustaining the Global Geodetic Reference Frame: A Plan to Help Achieve the Long-Term Accuracy and Accessibility of the Global Geodetic Reference Frame. E/C.20/2021/7/Add.2. 2021. Available online: https://ggim.un.org/meetings/GGIM-committee/11th-Session/documents/E-C.20-2021-7-Add-2_Position_Paper_on_Sustaining_the_GGRF_29Jul2021.pdf (accessed on 13 May 2022).
12. United Nations General Assembly Resolution, A Global Geodetic Reference Frame for Sustainable Development. 2015. Available online: https://ggim.un.org/documents/A_RES_69_266_E.pdf (accessed on 13 May 2022).
13. International VLBI Service for Geodesy and Astrometry, Terms of Reference. 1998. Available online: <https://ivsc.gsfc.nasa.gov/about/org/documents/tor981020.html> (accessed on 13 May 2022).
14. Sovers, O.J.; Jacobs, C.S.; Lanyi, G.E. MODEST: A Tool for Geodesy and Astrometry. In Proceedings of the International VLBI Service for Geodesy and Astrometry 2004 General Meeting, Ottawa, ON, Canada, 9–11 February 2004. Available online: <https://articles.adsabs.harvard.edu/pdf/2004ivsg.conf..272S> (accessed on 13 May 2022).
15. Petit, G.; Luzum, B. (Eds.) *IERS Conventions 2010, IERS Technical Note 36*; Verlag des Bundesamts für Kartographie und Geodäsie: Frankfurt am Main, Germany, 2010; p. 179, ISBN 3-89888-989-6. Available online: <https://www.iers.org/IERS/EN/Publications/TechnicalNotes/tn36.html-1.htm?nn=94912> (accessed on 13 May 2022).
16. IAU Resolution B2 on The Third Realization of the International Celestial Reference Frame. In Proceedings of the XXX IAU General Assembly, Vienna, Austria, 20–31 August 2018. Available online: https://www.iau.org/static/resolutions/IAU2018_ResolB2_English.pdf (accessed on 13 May 2022).
17. MacMillan, D.S.; Fey, A.; Gipson, J.M.; Gordon, D.; Jacobs, C.S.; Krásná, H.; Lambert, S.B.; Malkin, Z.; Titov, O.; Wang, G.; et al. Galactocentric acceleration in VLBI analysis: Findings of IVS WG8. *Astron. Astrophys.* **2019**, *630*, A93. Available online: https://www.aanda.org/articles/aa/full_html/2019/10/aa35379-19/aa35379-19.html (accessed on 13 May 2022). [[CrossRef](#)]
18. Treuhaft, R.N.; Lanyi, G.E. The effect of the dynamic wet troposphere on radio interferometric measurements. *Radio Sci.* **1987**, *22*, 251–265. Available online: <https://agupubs.onlinelibrary.wiley.com/doi/abs/10.1029/RS022i002p00251> (accessed on 13 May 2022). [[CrossRef](#)]
19. Charlot, P. Radio-Source Structure in Astrometric and Geodetic Very Long Baseline Interferometry. *Astron. J.* **1990**, *99*, 1309–1326. Available online: <https://articles.adsabs.harvard.edu/pdf/1990AJ.....99.1309C> (accessed on 13 May 2022). [[CrossRef](#)]

20. Gordon, D.; de Witt, A.; Jacobs, C.S. Current CRF Status at X/S and K Bands. In Proceedings of the 12th IVS General Meeting, Helsinki, Finland, 28 March–1 April 2022. Available online: https://www.maanmittauslaitos.fi/sites/maanmittauslaitos.fi/files/attachments/2022/03/Abstarct_book_2022.pdf (accessed on 13 May 2022).
21. Jacobs, C.S.; Horiuchi, S.; Snedeker, L.G.; Firre, D.; Murata, Y.; Takeuchi, H.; Uchimura, T.; Asmar, S. The JPL 2022a X/Ka Celestial Reference Frame. In Proceedings of the 12th IVS General Meeting, Helsinki, Finland, 28 March–1 April 2022. Available online: https://www.maanmittauslaitos.fi/sites/maanmittauslaitos.fi/files/attachments/2022/03/Abstarct_book_2022.pdf (accessed on 13 May 2022).
22. de Witt, A.; Jacobs, C.S.; Gordon, D.; Quick, J.; McCallum, J.; Krásná, H.; Soja, B.; Le Bail, K.; Horiuchi, S. K-band Celestial Reference Frame: Roadmap. In Proceedings of the Journées 2019, Astronomy, Earth Rotation and Reference Systems in the Gaia Era, Paris, France, 2–9 October 2019. Available online: https://syrtre.obspm.fr/astro/journees2019/journees_pdf/SessionIII_1/DE (accessed on 13 May 2022).
23. Jacobs, C.S.; Samoska, L.; Kooi, J.; Bowen, J.; Fung, A.; Manthena, R.; Lazio, J.; Firre, D.; Dugast, M.; De Vicente, J.; et al. X/Ka (8.4/32 GHz) Celestial Frame: Roadmap to the future. In Proceedings of the Journées 2019, Astronomy, Earth Rotation and Reference Systems in the Gaia Era, Paris, France, 2–9 October 2019. Available online: https://syrtre.obspm.fr/astro/journees2019/journees_pdf/SessionIII_1/JACOBS_Christopher.pdf (accessed on 13 May 2022).
24. de Witt, A.; Basu, S.; Charlot, P.; Gordon, D.; Jacobs, C.S.; Johnson, M.; Krásná, H.; Le Bail, K.; Shu, F.; Titov, O.; et al. Improving the S/X Celestial Reference Frame in the South: A Status Update. In Proceedings of the 25th Working Meeting of the European VLBI Group for Geodesy and Astrometry, Virtual, 14–18 March 2021. Available online: https://www.oso.chalmers.se/evga/25_EVGA_2021_Cyberspace.pdf (accessed on 13 May 2022).
25. Collioud, A.; Charlot, P. The Second Version of the Bordeaux VLBI Image Database (BVID). In Proceedings of the 24th European VLBI Group for Geodesy and Astrometry Working Meeting, Las Palmas de Gran Canaria, Spain, 17–19 March 2019; pp. 219–223. Available online: https://www.oan.es/evga2019/24_EVGA_2019_Las_Palmas.pdf (accessed on 13 May 2022).
26. Hunt, L.; Johnson, M.; Fey, A.; Gordon, D.; Spitzak, J. Imaging Over 3000 Quasars That Are a Part of the International Celestial Reference Frame. In Proceedings of the American Astronomical Society Meeting Abstracts, Honolulu, HI, USA, 4–8 January 2020; Volume 235, p. 305.30. Available online: <https://assets.pubpub.org/rynkb0j6/71582749259388.pdf#abs305.30> (accessed on 13 May 2022).
27. de Witt, A.; Jacobs, C.S.; Gordon, D.; Bietenholz, M.; Nickola, M.; Bertarini, A. The Celestial Reference Frame at K-band: Imaging. I. First 28 Epochs of K-band Images. *Astron. J.* 2022, *under review*.
28. Hunt, L.; de Witt, A.; Gordon, D.; Jacobs, C.S. Comparing Images of ICRF Sources at S, X, K, and Q-Bands. In Proceedings of the 12th IVS General Meeting, Helsinki, Finland, 27 March–1 April 2022. Available online: https://www.maanmittauslaitos.fi/sites/maanmittauslaitos.fi/files/attachments/2022/03/Abstarct_book_2022.pdf (accessed on 13 May 2022).
29. Xu, M.H.; Savolainen, T.; Anderson, J.M.; Kareinen, N.; Zubko, N.; Lunz, S.; Schuh, H. Impacts of the image alignment over frequency for VLBI Global Observing System. *arXiv* 2021, arXiv:2109.09315. Available online: <https://arxiv.org/pdf/2109.09315.pdf> (accessed on 13 May 2022).
30. Xu, M.H.; Savolainen, T.; Zubko, N.; Poutanen, M.; Lunz, S.; Schuh, H.; Wang, G.L. Imaging VGOS Observations and Investigating Source Structure Effects. *J. Geophys. Res. (Solid Earth)* 2021, 126, e21238. Available online: <https://agupubs.onlinelibrary.wiley.com/doi/10.1029/2020JB021238> (accessed on 13 May 2022). [CrossRef]
31. Klioner, S.A.; Lindgren, L.; Mignard, F.; Hernández, J.; Ramos-Lerate, M.; Bastian, U.; Biermann, M.; Bombrun, A.; de Torres, A.; Gerlach, E.; et al. Gaia Early Data Release 3: The celestial reference frame (Gaia-CRF3). *arXiv* 2022, arXiv:2204.12574. Available online: <https://ui.adsabs.harvard.edu/abs/2022arXiv220412574G/abstract> (accessed on 13 May 2022).
32. IAU Resolution B3: On the Gaia Celestial Reference Frame. In Resolutions presented to the XXXIst General Assembly. 2021. Available online: <https://www.iau.org/static/archives/announcements/pdf/ann21040c.pdf> (accessed on 13 May 2022).
33. Jansky, K.G. Radio Waves from Outside the Solar System. *Nature* 1933, 132, 66. Available online: <https://www.nature.com/articles/132066a0> (accessed on 13 May 2022). [CrossRef]
34. Carr, T.D.; May, J.; Olson, C.N.; Walls, G.F. Post-detector correlation interferometry of Jupiter at 18 Mc/s. *IEEE Nereid* 1965, 7, 222.
35. Bare, C.; Clark, B.G.; Kellermann, K.I.; Cohen, M.H.; Jauncey, D.L. Interferometer Experiment with Independent Local Oscillators. *Science* 1967, 157, 189–191. Available online: <https://www.science.org/doi/10.1126/science.157.3785.189> (accessed on 13 May 2022). [CrossRef]
36. Broten, N.W.; Locke, J.L.; Legg, T.H.; McLeish, C.W.; Richards, R.S. Observations of Quasars using Interferometer Baselines up to 3074 km. *Nature* 1967, 215, 38. Available online: <https://www.nature.com/articles/215038a0> (accessed on 13 May 2022). [CrossRef]
37. Matveyenko, L. Early VLBI in the USSR. In Proceedings of the Science, Resolving The Sky—Radio Interferometry: Past, Present and Future, Manchester, UK, 17–20 April 2012. Available online: <https://pos.sissa.it/163/004/pdf> (accessed on 13 May 2022).
38. May, J.; Carr, T.D. Interferometry of Jupiter at 18 Mc/s. *Q. J. Fla. Acad. Sci.* 1967, 30, 1–9. Available online: <https://www.jstor.org/stable/24314980> (accessed on 13 May 2022).
39. Moran, J.M.; Crowther, P.P.; Burke, B.F.; Barrett, A.H.; Rogers, A.E.E.; Ball, J.A.; Carter, J.C.; Bare, C.C. Spectral Line Interferometry with Independent Time Standards at Stations Separated by 845 Kilometers. *Science* 1967, 157, 676–677. Available online: <https://www.science.org/doi/10.1126/science.157.3789.676> (accessed on 13 May 2022). [CrossRef]

40. Cohen, M.H.; Jauncey, D.L.; Kellermann, K.I.; Clark, B.G. Radio Interferometry at One-Thousandth Second of Arc. *Science* **1968**, *162*, 88–94. Available online: <https://www.science.org/doi/10.1126/science.162.3849.88> (accessed on 13 May 2022). [CrossRef]
41. Kellermann, K.I.; Cohen, M.H. The origin and evolution of the NRAO-Cornell VLBI system. *J. R. Astron. Soc. Can.* **1988**, *82*, 248–265. Available online: <https://articles.adsabs.harvard.edu/pdf/1988JRASC..82..248K> (accessed on 13 May 2022).
42. Kellerman, K.I.; Moran, J.M. The Development of High-Resolution Imaging in Radio Astronomy. *Annu. Rev. Astron. Astrophys.* **2001**, *39*, 457–509. Available online: <https://www.annualreviews.org/doi/pdf/10.1146/annurev.astro.39.1.457> (accessed on 13 May 2022). [CrossRef]
43. Clark, B.G. A Review of the History of VLBI. In *Radio Astronomy at the Fringe*; Zensus, J.A., Cohen, M.H., Ros, E., Eds.; ASP Conference Series; Astronomical Society of the Pacific: San Francisco, CA, USA, 2003; Volume 300. Available online: <http://aspbooks.org/publications/300/1.pdf> (accessed on 13 May 2022).
44. Cohen, M.H. Accurate Positions for Radio Sources. *Astrophys. Lett.* **1972**, *12*, 81. Available online: <https://articles.adsabs.harvard.edu/pdf/1972ApL....12..81C> (accessed on 13 May 2022).
45. Hinteregger, H.F.; Shapiro, I.I.; Robertson, D.S.; Knight, C.A.; Ergas, R.A.; Whitney, A.R.; Rogers, A.E.E.; Moran, J.M.; Clark, T.A.; Burke, B.F. Precision Geodesy via Radio Interferometry. *Science* **1972**, *178*, 396–398. Available online: <https://www.science.org/doi/10.1126/science.178.4059.396> (accessed on 13 May 2022). [CrossRef] [PubMed]
46. Rogers, A.E.E.; Counselman, C.C., III; Hinteregger, H.F.; Knight, C.A.; Robertson, D.S.; Shapiro, I.I.; Whitney, A.R.; Clark, T.A. Extragalactic Radio Sources: Accurate Positions from Very-Long Interferometry Observations. *Astrophys. J.* **1973**, *186*, 801–806. Available online: <https://articles.adsabs.harvard.edu/pdf/1973ApJ...186..801R> (accessed on 13 May 2022). [CrossRef]
47. Clark, T.A.; Hutton, L.K.; Marandino, G.E.; Counselman, C.C.; Robertson, D.S.; Shapiro, I.I.; Wittels, J.J.; Hinteregger, H.F.; Knight, C.A.; Rogers, A.E.E.; et al. Radio source positions from very-long-baseline interferometry observations. *Astron. J.* **1976**, *81*, 599–603. Available online: <https://articles.adsabs.harvard.edu/pdf/1976AJ.....81..599C> (accessed on 13 May 2022). [CrossRef]
48. Preston, R.A.; Slade, M.A.; Williams, J.G.; Fanselow, J.L.; Harris, A.W. Development of a VLBI reference co-ordinate system. *Bull. Am. Astron. Soc.* **1976**, *8*, 432. Available online: <https://articles.adsabs.harvard.edu/pdf/1976BAAS...8..432P> (accessed on 13 May 2022).
49. Fanselow, J.L.; Sovers, O.J.; Thomas, J.B.; Purcell, G.H., Jr.; Cohen, E.J.; Rogstad, D.H.; Skjerve, L.J.; Spitzmesser, D.J. Radio interferometric determination of source positions utilizing deep space network antennas—1971 to 1980. *Astron. J.* **1984**, *89*, 987–998. Available online: <https://articles.adsabs.harvard.edu/pdf/1984AJ.....89..987F> (accessed on 13 May 2022). [CrossRef]
50. Fricke, W.; Schwan, H.; Lederle, T.; Bastian, U.; Bien, R.; Burkhardt, G.; Du Mont, B.; Hering, R.; Jährling, R.; Jahreiß, H.; et al. Fifth Fundamental Catalogue (FK5). Part 1. The Basic Fundamental Stars. *Veröffentlichungen Des Astron.-Rechen-Instituts Heidelb.* **1988**, *32*, 1–106. Available online: <https://ui.adsabs.harvard.edu/abs/1988VeARL..32....1F/abstract> (accessed on 13 May 2022).
51. Ma, C.; Clark, T.A.; Ryan, J.W.; Herring, T.A.; Shapiro, I.I.; Corey, B.E.; Hinteregger, H.F.; Rogers, A.E.E.; Whitney, A.R.; Knight, C.A.; et al. Radio-source positions from VLBI. *Astron. J.* **1986**, *92*, 1020–1029. Available online: <https://articles.adsabs.harvard.edu/pdf/1986AJ.....92.1020M> (accessed on 13 May 2022). [CrossRef]
52. Robertson, D.S.; Fallon, F.W.; Carter, W.E. Celestial reference coordinate systems: Submilliarcsecond precision demonstrated with VLBI observations. *Astron. J.* **1986**, *91*, 1456–1462. Available online: <https://articles.adsabs.harvard.edu/pdf/1986AJ.....91.1456R> (accessed on 13 May 2022). [CrossRef]
53. Sovers, O.J.; Edwards, C.D.; Jacobs, C.S.; Lanyi, G.E.; Liewer, K.M.; Treuhaft, R.N. Astrometric Results of 1978–1985 Deep Space Network Radio Interferometry: The JPL 1987-1 Extragalactic Source Catalog. *Astron. J.* **1988**, *95*, 1647. Available online: <https://articles.adsabs.harvard.edu/pdf/1988AJ.....95.1647S> (accessed on 13 May 2022). [CrossRef]
54. Hazard, C.; Sutton, J.; Argue, A.N.; Kenworthy, C.M.; Morrison, L.V.; Murray, C.A. Accurate Radio and Optical Positions of 3C273B. *Nat. Phys. Sci.* **1971**, *233*, 89–91. Available online: <https://www.nature.com/articles/physci233089a0> (accessed on 13 May 2022). [CrossRef]
55. Arias, E.F.; Feissel, M.; Lestrade, J.F. *BIH Annual Report for 1987*; Sections B21-C11; BIH: Paris, France, 1987. Available online: https://webtai.bipm.org/ftp/pub/tai/annual-reports/bih-annual-report/BIH_1987.pdf (accessed on 13 May 2022).
56. International Earth Rotation Service (IERS). *Annual Report for 1988*; Observatoire de Paris (France); Central Bureau de l’IERS: Frankfurt am Main, Germany, 1989; ISBN 2-900340-01-0.
57. International Earth Rotation Service (IERS). *Annual Report for 1989*; Observatoire de Paris (France); Central Bureau de l’IERS: Frankfurt am Main, Germany, 1990; ISBN 2-900340-02-0. Available online: <https://ui.adsabs.harvard.edu/abs/1990iers.book...../abstract> (accessed on 13 May 2022).
58. International Earth Rotation Service (IERS). *Annual Report for 1990*; Observatoire de Paris (France); Central Bureau of IERS: Frankfurt am Main, Germany, 1991; ISBN 2-900340-03-9. Available online: <https://ui.adsabs.harvard.edu/abs/1991iers.book...../abstract> (accessed on 13 May 2022).
59. International Earth Rotation Service (IERS). *Annual Report for 1991*; Observatoire de Paris (France); Central Bureau of IERS: Frankfurt am Main, Germany, 1992; ISBN 2-900340-04-7. Available online: <https://ui.adsabs.harvard.edu/abs/1992iers.book...../abstract> (accessed on 13 May 2022).
60. International Earth Rotation Service (IERS). *1992 IERS (International Earth Rotation Service) Annual Report*; Observatoire de Paris (France); Central Bureau of IERS: Frankfurt am Main, Germany, 1993; ISBN 2-900340-05-5. Available online: <https://ui.adsabs.harvard.edu/abs/1993iers.book...../abstract> (accessed on 13 May 2022).

61. International Earth Rotation Service (IERS). 1993 *IERS (International Earth Rotation Service) Annual Report*; Observatoire de Paris (France); Central Bureau of IERS: Frankfurt am Main, Germany, 1994. Available online: <https://ui.adsabs.harvard.edu/abs/1994iers.bookQ...../abstract> (accessed on 13 May 2022).
62. Walter, H.G.; Sovers, O.J. *Astrometry of Fundamental Catalogues: The Evolution from Optical to Radio Reference Frames*; Springer: Berlin/Heidelberg, Germany, 2000. Available online: <https://link.springer.com/book/10.1007/978-3-642-57260-9> (accessed on 13 May 2022).
63. IAU Resolution C1. 1988. Available online: https://iau.org/static/resolutions/IAU1988_French.pdf (accessed on 13 May 2022).
64. IAU Resolution A4. 1991. Available online: https://www.iau.org/static/resolutions/IAU1991_French.pdf (accessed on 13 May 2022).
65. IAU Resolution B5. 1994. Available online: https://www.iau.org/static/resolutions/IAU1994_French.pdf (accessed on 13 May 2022).
66. Lestrade, J.F.; Jones, D.L.; Preston, R.A.; Phillips, R.B.; Titus, M.A.; Kovalevsky, J.; Lindegren, L.; Hering, R.; Froeschle, M.; Falin, J.L.; et al. Preliminary link of the HIPPARCOS and VLBI reference frames. *Astron. Astrophys.* **1995**, *304*, 182. Available online: <https://articles.adsabs.harvard.edu/pdf/1995A> (accessed on 13 May 2022).
67. IAU Resolutions B2 (ICRS, ICRF), B3 (Relativistic Framework), B4 (Non-Rigid Earth Theory for Nutations), B5 (ICRS and Hipparcos), B6 (Relativity in Celestial Mechanics and Astrometry), XXIII General Assembly, Kyoto, Japan, 1997. Available online: https://www.iau.org/static/resolutions/IAU1997_French.pdf (accessed on 13 May 2022).
68. Charlot, P.; Boboltz, D.A.; Fey, A.L.; Fomalont, E.B.; Geldzahler, B.J.; Gordon, D.; Jacobs, C.S.; Lanyi, G.E.; Ma, C.; Naudet, C.J.; et al. The Celestial Reference Frame at 24 and 43 GHz. II. Imaging. *Astron. J.* **2010**, *139*, 1713–1770. Available online: <https://iopscience.iop.org/article/10.1088/0004-6256/139/5/1713> (accessed on 13 May 2022). [[CrossRef](#)]
69. Lanyi, G.E.; Boboltz, D.A.; Charlot, P.; Fey, A.L.; Fomalont, E.B.; Geldzahler, B.J.; Gordon, D.; Jacobs, C.S.; Ma, C.; Naudet, C.J.; et al. The Celestial Reference Frame at 24 and 43 GHz. I. Astrometry. *Astron. J.* **2010**, *139*, 1695–1712. Available online: <https://iopscience.iop.org/article/10.1088/0004-6256/139/5/1695> (accessed on 13 May 2022). [[CrossRef](#)]
70. de Witt, A.; Bertarini, A.; Horiuchi, S.; Jacobs, C.S.; Jung, T.; Lovell, J.E.J.; McCallum, J.N.; Quick, J.F.H.; Sohn, B.W.; Phillips, C.; et al. Completing the K-band Celestial Reference Frame in the Southern Hemisphere. In Proceedings of the 8th IVS General Meeting: VGOS: The New VLBI Network, Beijing, China, 2–7 March 2014; pp. 433–437. Available online: https://ivscc.gsfc.nasa.gov/publications/gm2014/093_deWitt_etal.pdf (accessed on 13 May 2022).
71. Reid, M.J.; Menten, K.M.; Brunthaler, A.; Zheng, X.W.; Dame, T.M.; Xu, Y.; Li, J.; Sakai, N.; Wu, Y.; Immer, K.; et al. Trigonometric Parallaxes of High-mass Star-forming Regions: Our View of the Milky Way. *Astrophys. J.* **2019**, *885*, 131. Available online: <https://iopscience.iop.org/article/10.3847/1538-4357/ab4a11> (accessed on 13 May 2022). [[CrossRef](#)]
72. Gordon, D.; de Witt, A.; Jacobs, C.S. ICRF3 Position and Proper Motion of Sagittarius A* from VLBA Absolute Astrometry. In Proceedings of the 12th IVS General Meeting, Helsinki, Finland, 28 March–1 April 2022. Available online: https://www.maanmittauslaitos.fi/sites/maanmittauslaitos.fi/files/attachments/2022/03/Abstarct_book_2022.pdf (accessed on 13 May 2022).
73. Shambayati, S.; Morabito, D.; Border, J.S.; Davarian, F.; Lee, D.; Mendoza, R.; Britcliffe, M.S.; Weinreb, S. Mars Reconnaissance Orbiter Ka-band (32 GHz) Demonstration: Cruise Phase Operations. In Proceedings of the AIAA 9th International Conference on Space Operations (SpaceOps), Rome, Italy, 19–23 June 2006. Available online: <http://hdl.handle.net/2014/39654> (accessed on 13 May 2022).
74. Jacobs, C.S.; de Vicente, J.; Dugast, M.; García-Miró, C.; Goodhart, C.E.; Horiuchi, S.; Lowe, S.T.; Maddè, R.; Micolino, M.; Naudet, C.J.; et al. Extending the X/Ka Celestial Reference Frame over the South Polar Cap: Results from combined NASA-ESA Deep Space Network baselines to Malargüe, Argentina. In Proceedings of the 21st Meeting of the EVGA, Espoo, Finland, 5–8 March 2013. Available online: <https://ui.adsabs.harvard.edu/abs/2013evga.confE...1J/abstract> (accessed on 13 May 2022).
75. Jacobs, C.S.; Murata, Y.; Takeuchi, H.; Firee, D.; Asmar, S.; Uchimura, T.; Numata, K. X/Ka Network Enhanced by Misasa, Japan’s 54-meter antenna. In Proceedings of the 25th Working Meeting of the European VLBI Group for Geodesy and Astrometry, Virtual, 14–18 March 2021. Available online: <https://ui.adsabs.harvard.edu/abs/2021evga.confE...3J/abstract> (accessed on 13 May 2022).
76. Mignard, F.; Klioner, S.A.; Lindegren, L.; Hernandez, J.; Bastian, U.; Bombrun, A.; Hobbs, D.; Lammers, U.; Michalik, D.; Ramos-Lerate, M.; et al. Gaia Data Release 2: The celestial reference frame (Gaia-CRF2). *Astron. Astrophys.* **2018**, *616*, A14. Available online: https://www.aanda.org/articles/aa/full_html/2018/08/aa32916-18/aa32916-18.html (accessed on 13 May 2022).
77. Park, R.S.; Folkner, W.M.; Williams, J.G.; Boggs, D.H. The JPL Planetary and Lunar Ephemerides DE440 and DE441. *Astron. J.* **2021**, *161*, 105. Available online: <https://iopscience.iop.org/article/10.3847/1538-3881/abd414> (accessed on 13 May 2022). [[CrossRef](#)]
78. Beasley, A.J.; Conway, J.E. VLBI Phase Referencing. In *Very Long Baseline Interferometry and the VLBA*; Zensus, J.A., Diamond, P.J., Napier, P.J., Eds.; Astronomical Society of the Pacific Conference Series; Astronomical Society of the Pacific: San Francisco, CA, USA, 1995; Volume 82, p. 327. Available online: <https://articles.adsabs.harvard.edu/pdf/1995ASPC...82..327B> (accessed on 13 May 2022).
79. Rioja, M.J.; Dodson, R. Precise radio astrometry and new developments for the next-generation of instruments. *Astron. Astrophys. Rev.* **2020**, *28*, 6. Available online: <https://link.springer.com/article/10.1007/s00159-020-00126-z> (accessed on 13 May 2022). [[CrossRef](#)]

80. Fomalont, E.; Kopeikin, S.; Lanyi, G.; Benson, J. Progress in Measurements of the Gravitational Bending of Radio Waves Using the VLBA. *Astrophys. J.* **2009**, *699*, 1395–1402. Available online: <https://iopscience.iop.org/article/10.1088/0004-637X/699/2/1395> (accessed on 13 May 2022). [CrossRef]
81. Prusti, T.; De Bruijne, J.H.; Brown, A.G.; Vallenari, A.; Babusiaux, C.; Bailer-Jones, C.A.; Bastian, U.; Biermann, M.; Evans, D.W.; Eyer, L.; et al. The Gaia mission. *Astron. Astrophys.* **2016**, *595*, A1. Available online: https://www.aanda.org/articles/aa/full_html/2016/11/aa29272-16/aa29272-16.html (accessed on 13 May 2022).
82. Altamimi, Z.; Rebischung, P.; Collilieux, X.; Metivier, L.; Chanard, K.; Teyssendier-de-la-Serve, M. Preparatory analysis and development for the ITRF2020. In Proceedings of the EGU General Assembly Conference Abstracts 2021, EGU21-2056, Virtual, 19–30 April 2021. Available online: <https://meetingorganizer.copernicus.org/EGU21/EGU21-2056.html> (accessed on 13 May 2022).
83. Altamimi, Z.; Rebischung, P.; Collilieux, X.; Metivier, L.; Chanard, K. ITRF2020 and the IVS Contribution. In Proceedings of the 12th IVS General Meeting, Helsinki, Finland, 28 March–1 April 2022. Available online: https://www.maanmittauslaitos.fi/sites/maanmittauslaitos.fi/files/attachments/2022/03/Abstarct_book_2022.pdf (accessed on 13 May 2022).
84. Sovers, O.J.; Fanelow, J.L.; Jacobs, C.S. Astrometry and geodesy with radio interferometry: Experiments, models, results. *Rev. Mod. Phys.* **1998**, *70*, 1393–1454. Available online: <https://journals.aps.org/rmp/abstract/10.1103/RevModPhys.70.1393> (accessed on 13 May 2022). [CrossRef]
85. Jacobs, C.S.; Heflin, M.B.; Lanyi, G.E.; Sovers, O.J.; Steppe, J.A. Rotational Alignment Altered by Source Position Correlations. In Proceedings of the Sixth General Meeting of the International VLBI Service for Geodesy and Astrometry 2010, Hobart, Australia, 7–13 February 2010; NASA/CP 2010-215864; Behrend, D., Baver, K.D., Eds.; Volume 305. Available online: <https://ivsc.gsfc.nasa.gov/publications/gm2010/jacobs2.pdf> (accessed on 13 May 2022).
86. Xu, M.H.; Anderson, J.M.; Heinkelmann, R.; Lunz, S.; Schuh, H.; Wang, G.L. Structure Effects for 3417 Celestial Reference Frame Radio Sources. *Astrophys. J. Suppl. Ser.* **2019**, *242*, 5. Available online: <https://iopscience.iop.org/article/10.3847/1538-4365/ab16ea/pdf> (accessed on 13 May 2022). [CrossRef]
87. Gattano, C.; Lambert, S.B.; Le Bail, K. Extragalactic radio source stability and VLBI celestial reference frame: Insights from the Allan standard deviation. *Astron. Astrophys.* **2018**, *618*, A80. Available online: <https://www.aanda.org/articles/aa/pdf/2018/10/aa33430-18.pdf> (accessed on 13 May 2022). [CrossRef]
88. Charlot, P. Modeling Radio Source Structure for Improved VLBI Data Analysis. In Proceedings of the IVS 2002 General Meeting Proceedings, Tsukuba, Japan, 4–7 February 2002; NASA/CP-2002-210002; Vandenberg, N.R., Baver, K.D., Eds.; pp. 233–242. Available online: <https://articles.adsabs.harvard.edu/pdf/2002ivsg.conf.233C> (accessed on 13 May 2022).
89. IAU Resolution B3 on The Second Realization of the International Celestial Reference Frame. In Proceedings of the XXVII IAU General Assembly, Rio de Janeiro, Brazil, 2–15 August 2009. Available online: https://www.iau.org/static/resolutions/IAU2009_English.pdf (accessed on 13 May 2022).
90. Jacobs, C.S.; Clark, J.E.; García-Míro, C.; Horiuchi, S.; Romero-Wolf, A.; Snedeker, L.; and Sotuela, I. Celestial Reference Frame at X/Ka-Band (8.4/32 GHz) for Deep Space Navigation. In Proceedings of the 23rd Symposium on Space Flight Dynamics, Pasadena, CA, USA, 29 October–2 November 2012. Available online: https://issfd.org/ISSFD_2012/ISSFD23_OD1_1.pdf (accessed on 13 May 2022).
91. Fey, A.L.; Clegg, A.W.; Fomalont, E.B. VLBA Observations of Radio Reference Frame Sources. I. *Astrophys. J. Suppl. Ser.* **1996**, *105*, 299–330. Available online: <https://articles.adsabs.harvard.edu/pdf/1996ApJS.105..299F> (accessed on 13 May 2022). [CrossRef]
92. Fey, A.L.; Charlot, P. VLBA Observations of Radio Reference Frame Sources. II. Astrometric Suitability Based on Observed Structure. *Astrophys. J. Suppl. Ser.* **1997**, *111*, 95–142. Available online: <https://iopscience.iop.org/article/10.1086/313017> (accessed on 13 May 2022). [CrossRef]
93. Fey, A.L.; Charlot, P. VLBA Observations of Radio Reference Frame Sources. III. Astrometric Suitability of an Additional 225 Sources. *Astrophys. J. Suppl. Ser.* **2000**, *128*, 17–83. Available online: <https://iopscience.iop.org/article/10.1086/313382> (accessed on 13 May 2022). [CrossRef]
94. Charlot, P. Astrophysical Stability of Radio Sources and Implication for the Realization of the Next ICRF. In Proceedings of the Fifth IVS General Meeting, Helsinki, Finland, 27 March–1 April 2008; Finkelstein, A., Behrend, D., Eds.; pp. 345–354. Available online: <https://ivsc.gsfc.nasa.gov/publications/gm2008/charlot.pdf> (accessed on 13 May 2022).
95. Liu, N.; Lambert, S.B.; Charlot, P.; Zhu, Z.; Liu, J.C.; Jiang, N.; Wan, X.S.; Ding, C.Y. Comparison of multifrequency positions of extragalactic sources from ICRF3 and Gaia EDR3. *Astron. Astrophys.* **2021**, *652*, A87. Available online: https://www.aanda.org/articles/aa/full_html/2021/08/aa38179-20/aa38179-20.html (accessed on 13 May 2022). [CrossRef]
96. Petrov, L.; Kovalev, Y.Y.; Plavin, A.V. A quantitative analysis of systematic differences in the positions and proper motions of Gaia DR2 with respect to VLBI. *Mon. Not. R. Astron. Soc.* **2019**, *482*, 3023–3031. Available online: <https://academic.oup.com/mnras/article/482/3/3023/5187384> (accessed on 13 May 2022). [CrossRef]
97. Plavin, A.V.; Kovalev, Y.Y.; Petrov, L. Dissecting the AGN Disk-Jet System with Joint VLBI-Gaia Analysis. *Astrophys. J.* **2019**, *871*, 143. Available online: <https://iopscience.iop.org/article/10.3847/1538-4357/aaf650> (accessed on 13 May 2022). [CrossRef]
98. Lambert, S.; Liu, N.; Arias, E.F.; Barache, C.; Souchay, J.; Taris, F.; Liu, J.C.; Zhu, Z. Parsec-scale alignments of radio-optical offsets with jets in AGNs from multifrequency geodetic VLBI, Gaia EDR3, and the MOJAVE program. *Astron. Astrophys.* **2021**, *651*, A64. Available online: https://www.aanda.org/articles/aa/full_html/2021/07/aa40652-21/aa40652-21.html (accessed on 13 May 2022). [CrossRef]

99. Collioud, A.; Charlot, P.; Lambert, S. Exploring Source Structure with the Bordeaux VLBI Image Database—Comparing Jet Directions with Optical Radio Offset Vectors. In Proceedings of the 12th IVS General Meeting, Helsinki, Finland, 28 March–1 April 2022. Available online: https://www.maanmittauslaitos.fi/sites/maanmittauslaitos.fi/files/attachments/2022/03/Abstarct_book_2022.pdf (accessed on 13 May 2022).
100. de Witt, A.; Jacobs, C.; Gordon, D.; Hunt, L.; Johnson, M. Sources with Significant Astrometric Offsets Between the S/X and K-band Celestial Frames. In Proceedings of the 12th IVS General Meeting, Helsinki, Finland, 28 March–1 April 2022. Available online: https://www.maanmittauslaitos.fi/sites/maanmittauslaitos.fi/files/attachments/2022/03/Abstarct_book_2022.pdf (accessed on 13 May 2022).
101. Laboratoire d’Astrophysique de Bordeaux (LAB), Bordeaux VLBI Image Database (BVID). Available online: <http://bvid.astrophys.u-bordeaux.fr> (accessed on 13 May 2022).
102. Petrov, L. Radio Fundamental Catalog. Astro-geo Center. Available online: <http://astrogeo.org/rfc/> (accessed on 13 May 2022).
103. U.S. Naval Observatory Fundamental Reference Image Data Archive (FRIDA). Available online: https://crf.usno.navy.mil/data_products/FRIDA/frida.html (accessed on 13 May 2022).
104. Schartner, M.; Böhm, J. VieSched++: A New VLBI Scheduling Software for Geodesy and Astrometry. *Publ. Astron. Soc. Pac.* **2019**, *131*, 084501. Available online: <https://iopscience.iop.org/article/10.1088/1538-3873/ab1820/pdf> (accessed on 13 May 2022). [CrossRef]
105. Basu, S.; de Witt, A.; Gattano, C. Source Structure and Position Stability of Celestial Reference Frame Sources in the Deep South. In Proceedings of the 25th Working Meeting of the European VLBI Group for Geodesy and Astrometry, Virtual, 14–18 March 2021; Haas, R., Ed. Available online: https://www.oso.chalmers.se/evga/25_EVGA_2021_Cyberspace.pdf (accessed on 13 May 2022).
106. Soja, B.; Jacobs, C.S.; Runge, T.; Naudet, C.; Gross, R.; de Witt, A.; Gordon, D.; Quick, J.; McCallum, J.; Krásná, H. Ionospheric Calibration for K-Band Celestial Reference Frames. In Proceedings of the 24th European VLBI Group for Geodesy and Astrometry Working Meeting, Las Palmas, Gran Canaria, Spain, 17–19 March 2019; Haas, R., Garcia-Espada, S., López-Fernández, J.A., Eds. Available online: https://www.oan.es/evga2019/EVGA2019_PDF/O316_EVGA2019_Soja.pdf (accessed on 13 May 2022).
107. Lister, M.L.; Homan, D.C. MOJAVE: Monitoring of Jets in Active Galactic Nuclei with VLBA Experiments. I. First-Epoch 15 GHz Linear Polarization Images. *Astron. J.* **2005**, *130*, 1389–1417. Available online: <https://iopscience.iop.org/article/10.1086/432969/pdf> (accessed on 13 May 2022). [CrossRef]
108. Boccardi, B.; Krichbaum, T.P.; Ros, E.; Zensus, J.A. Radio observations of active galactic nuclei with mm-VLBI. *Astron. Astrophys. Rev.* **2017**, *25*, 4. Available online: <https://link.springer.com/article/10.1007/s00159-017-0105-6> (accessed on 13 May 2022). [CrossRef]
109. Kurtz, S.E.; Stander, T.; de Villiers, D.I.L.; Cerfonteyn, W.; de Witt, A.; Ferrusca Rodríguez, D.; Hiriart, D.; Hughes, D.H.; Jacobs, C.S.; Loinard, L.; et al. The potential for a K-band receiver on the Large Millimeter Telescope. In Proceedings of the Millimeter, Submillimeter, and Far-Infrared Detectors and Instrumentation for Astronomy X, SPIE Conference Series 11453, Virtual, 14–18 December 2020; Volume 11453, p. E40. Available online: <https://www.spiedigitallibrary.org/conference-proceedings-of-spie/11453/2563132/The-potential-for-a-K-band-receiver-on-the-Large/10.1117/12.2563132.full?SSO=1> (accessed on 13 May 2022).
110. Bourda, G.; Charlot, P. Preparing the VLBI Celestial Reference Frame for the Gaia Era: Observations of ICRF2 Sources to Improve the Astrometry of the Future Radio-Optical Transfer Sources. IVS Memorandum 2012-001v01. 2012. Available online: <https://ivscc.gsfc.nasa.gov/publications/memos/ivs-2012-001v01.pdf> (accessed on 13 May 2022).
111. Le Bail, K.; Gipson, J.M.; Gordon, D.; MacMillan, D.S.; Behrend, D.; Thomas, C.C.; Bolotin, S.; Himwich, W.E.; Bayer, K.D.; Corey, B.E.; et al. IVS Observation of ICRF2-Gaia Transfer Sources. *Astron. J.* **2016**, *151*, 79. Available online: <https://iopscience.iop.org/article/10.3847/0004-6256/151/3/79/pdf> (accessed on 13 May 2022). [CrossRef]
112. Charlot, P. Precision Astrometry: From VLBI to Gaia and SKA. In *The Square Kilometre Array: Paving the Way for the New 21st Century Radio Astronomy Paradigm*; Astrophysics and Space Science Proceedings; Barbosa, D., Anton, S., Gurvits, L., Maia, D., Eds.; Springer: Berlin/Heidelberg, Germany, 2012; pp. 85–95. Available online: https://link.springer.com/chapter/10.1007/978-3-642-22795-0_9 (accessed on 13 May 2022).
113. Paragi, Z.; Godfrey, L.; Reynolds, C.; Rioja, M.; Deller, A.; Zhang, B.; Gurvits, L.; Bietenholz, M.; Szomoru, A.; Bignall, H.; et al. Very Long Baseline Interferometry with the SKA. In Proceedings of the Advancing Astrophysics with the Square Kilometre Array (AASKA14), Naxos, Italy, 29 May 2015; Volume 143, p. 1412.5971. Available online: <https://pos.sissa.it/215/143/pdf> (accessed on 13 May 2022).
114. Charlot, P.; Garcia-Miró, C.; An, T.; Campbell, B.; Colomer, F.; de Witt, A.; Edwards, P.; Lambert, S. Looking into the future of the radio reference frame with SKA. In Proceedings of the Journées 2019—Astrometry, Earth Rotation and Reference Systems in the Gaia Era, Paris, France, 7–9 October 2019. Available online: <https://syrtte.obspm.fr/astro/journees2019/LATEX/JOURNEES2019.pdf> (accessed on 13 May 2022).
115. Schuh, H.; Behrend, D. VLBI: A fascinating technique for geodesy and astrometry. *J. Geodyn.* **2012**, *61*, 68–80. Available online: <https://www.sciencedirect.com/science/article/abs/pii/S0264370712001159?via> (accessed on 13 May 2022). [CrossRef]
116. McCallum, J.; McCallum, L. An S/X Compatible VGOS System for the AuScope Array. In Proceedings of the IVS 2018 General Meeting: Global Geodesy and the Role of VGOS—Fundamental to Sustainable Development, Longyearbyen, Norway, 3–8 June 2019. Available online: https://ivscc.gsfc.nasa.gov/publications/gm2018/27_mccallum_mccallum.pdf (accessed on 13 May 2022).

117. McCallum, L.; Chuan, L.C.; Krasna, L.; McCallum, J.; McCarthy, T.; Gruber, J.; Bohm, J.; Schartner, M.; Quick, J.; Weston, S. The Australian mixed-mode observing program. *J. Geod.* 2022, *under review*.
118. Soriano, M.; Kooi, J.; Bowen, J.; Fung, A.; Hoppe, D.; Mathena, R.; Abdulla, Z.; Samoska, L.; Jacobs, C.S. Simultaneous X- and Ka-Band Receiver for Astrometry and Navigation. In Proceedings of the 2021 XXXIVth General Assembly and Scientific Symposium of the International Union of Radio Science (URSI GASS, Rome, Italy, 28 August–4 September 2021). Available online: <https://www.ursi.org/proceedings/procGA21/papers/URSIGASS2021-We-J04-PM4-2.pdf> (accessed on 13 May 2022).
119. Charlot, P. IAU Working Group on Multi-waveband ICRF Terms of Reference. Available online: https://www.iau.org/static/science/scientific_bodies/working_groups/329/charter_icrf-multiwaveband-wg.pdf (accessed on 13 May 2022).
120. The Third Realization of the ICRF: ICRF-3. ICRF-3 Positions. Available online: <https://cdsarc.cds.unistra.fr/viz-bin/cat/J/A+A/644/A159> (accessed on 13 May 2022).
121. Napier, P.J. VLBA Design. In *ASP Conference Series: Very Long Baseline Interferometry and the VLBA*; Zensus, J.A., Diamond, P.J., Napier, P.J., Eds.; Astronomical Society of the Pacific: San Francisco, CA, USA, 1995; Volume 82, p. 59. Available online: <https://articles.adsabs.harvard.edu/pdf/1995ASPC...82...59N> (accessed on 13 May 2022).
122. Imbriale, W.A. Large Antennas of the Deep Space Network. In *Deep-Space Communication and Navigation Series, Monograph 4*; Jet Propulsion Laboratory, California Institute of Technology: Pasadena, CA, USA, 2002; Volume 4. Available online: https://descanso.jpl.nasa.gov/monograph/series4/Descanso_Mono4_web.pdf (accessed on 13 May 2022).
123. Vassallo, E.; Martin, R.; Madde, R.; Lanucara, M.; Besso, P.; Droll, P.; Galtie, G.; De Vicente, J. The European Space Agency's Deep-Space Antennas. *Proc. IEEE* 2007, *95*, 2111. Available online: <https://ieeexplore.ieee.org/document/4390046> (accessed on 13 May 2022). [[CrossRef](#)]